UNIVERSITY OF TURKU

Discovery of diagnostic biomarkers and targeted therapy for ductal carcinoma in situ (DCIS)

Institute of biomedicine
MDP in Biomedical Sciences, Drug Discovery and Development
Master's thesis

Author(s):
Emilia Huotari

Supervisor(s):
Emilia Peuhu, Docent
Laura Lehtinen, Senior Researcher

4.5.2024
Turku

Master's thesis

Subject: MDP in Biomedical Sciences, Drug Discovery and Development
Author(s): Emilia Huotari
Title: Discovery of diagnostic biomarkers and targeted therapy for ductal carcinoma in situ (DCIS)
Supervisor(s):
Emilia Peuhu, Academy Research Fellow, Docent
Laura Lehtinen, Senior Researcher, PhD
Number of pages: 61 pages
Date: 4.5.2024

Abstract

Breast cancer remains a significant public health problem affecting a remarkable proportion of women globally. Ductal carcinoma in situ (DCIS) is the most common non-invasive neoplasm found in mammography screenings and has an excellent prognosis in general. Nevertheless, approximately 10% of patient with high grade DCIS have a form of breast cancer known as neoductgenesis where cancerous duct-like structures of invasive nature are forming. Currently, neoductgenesis has no specific diagnosis and it is underdiagnosed as DCIS. Therefore, the aim of this thesis was to provide increased knowledge and histopathological markers for neoductgenesis. This thesis also aimed to test the efficacy of novel disulfide bridge-stabilized scFv antibody fragments of trastuzumab to improve the current treatment options of HER2-positive breast cancer. Imaging mass cytometry and immunofluorescence imaging were utilized to distinguish the spatial molecular features of selected breast cancer tissue samples that a pathologist had evaluated as high grade DCIS with or without neoductgenesis. The capacity of the ds-scFv-Fc antibody fragments to inhibit the proliferation of HER2-positive breast cancer cells was analyzed to evaluate whether the ds-scFv-Fc antibody fragments with potentially improved pharmacological properties have equal or even better efficacy compared to trastuzumab. This study identified several molecular features that appear specific to neoductgenesis and that help to explain its distinct and invasive nature. In the future, these findings have the potential to help the identification of the patients with neoductgenesis from DCIS in clinical histopathology. In addition, the ds-scFv-Fc antibody fragments demonstrated superior efficacy to inhibit the proliferation of trastuzumab-resistant HER2-positive breast cancer cells compared to trastuzumab, hence providing an alternative solution to overcome trastuzumab resistance. Further research is needed to validate the potential biomarkers for neoductgenesis in a larger sample cohort and to investigate the molecular action of the ds-scFv-Fc antibody fragments in trastuzumab-resistant cells.

Key words: Ductal carcinoma in situ, neoductgenesis, imaging mass cytometry, biomarker, HER2, single-chain variable fragment

Table of contents

1 Introduction

1.1 The structure and function of the mammary gland

The mammary gland has a significant role in the survival of mammalian offspring by producing milk. The human mammary gland is located in the chest wall and surrounded by fibrous stroma and adipose tissue (Figure 1A). The glandular tissue composed of an inner luminal epithelial cell layer and an outer myoepithelial cell layer (Figure 1B) is separated into 15-20 lobules, each of them having a collecting duct that connects to major lactiferous ducts. The major lactiferous ducts arise from the nipple and bifurcate into smaller ducts like branches of a tree. The collecting ducts eventually terminate into structures called terminal ductal lobular units (TDLUs) (Figure 1A, C), where the milk is produced by differentiated luminal cells during lactation (Wellings et al., 1975). Basement membrane forms an extracellular matrix (ECM) barrier between the mammary gland epithelium and stromal tissue. The ECM of the connective and adipose tissue supports the delicate structures of mammary gland forming the surrounding stroma (Figure 1B) (Biswas et al., 2022).

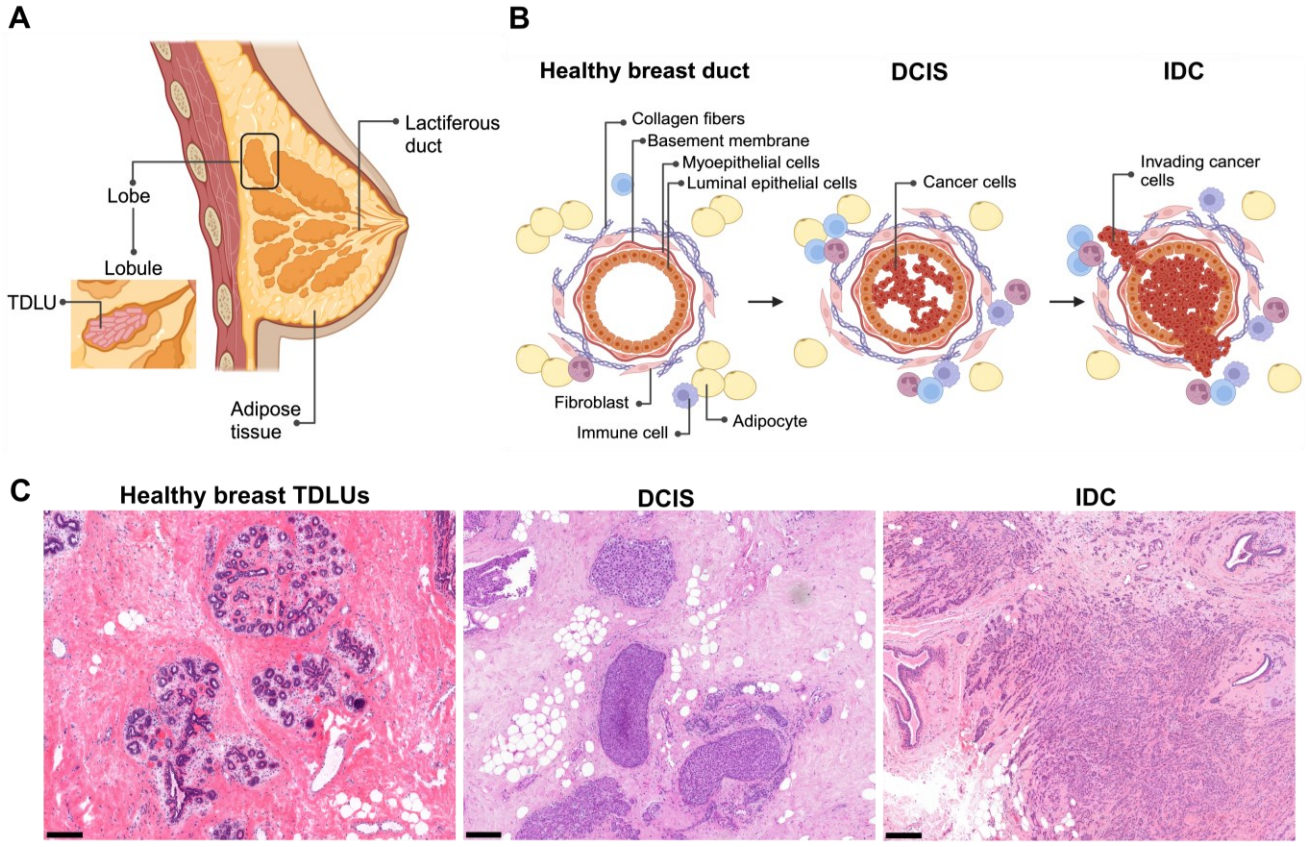

Figure 1. The structure of mammary gland. The human mammary gland is located in the chest wall, divided into 15-20 lobules, surrounded by fibrous stroma and adipose tissue (A). The major lactiferous ducts arise from the nipple and bifurcate into smaller ducts. The collecting ducts eventually terminate into TDLUs, where the milk is produced by differentiated luminal cells during lactation (A, C). The glandular mammary gland tissue consists of an inner luminal epithelial cell layer and an outer myoepithelial cell layer (B).

Basement membrane forms an ECM barrier between the mammary gland epithelium and stromal tissue. The ECM of the connective and adipose tissue supports the delicate structures of mammary gland forming the surrounding stroma (B). The majority of breast neoplasms develop in the TDLUs. The ductal carcinoma in situ (DCIS) is a non-invasive neoplasm where the abnormal epithelial cells fill the duct lumen but remain surrounded by myoepithelial cells and confined within the basement membrane (B, C). DCIS becomes invasive ductal carcinoma (IDC) when cancer cells across the basement membrane and spread to the surrounding stromal tissue (B, C). H&E-stained healthy human mammary tissue, DCIS and IDC (C). Scale bars: 200 μm. Figures A and B created in Biorender.

1.2 Breast cancer

Breast cancer remains a significant public health problem affecting a remarkable proportion of women globally. Breast cancer is the most commonly diagnosed malignancy as well as the leading cause of cancer deaths among women worldwide (Heer et al., 2020). Breast cancer is a very heterogeneous disease including a variable group of tumors that differ in terms of morphology, molecular features, behaviour and response to treatment (Rakha et al., 2023).

The majority of neoplasms of the breast develop in the TDLU (Figueroa et al., 2014). Breast cancer develops when DNA mutations in mammary epithelial cells lead to uncontrollable proliferation. In early-stage breast cancer, abnormal epithelial cells typically fill the duct lumen but remain surrounded by myoepithelial cells and confined within the basement membrane (Figure 1B, C). The non-invasive breast neoplasms are divided into ductal carcinoma in situ (DCIS) and lobular carcinoma in situ (LCIS) where DCIS is more common. The cancer is termed invasive when malignant cells have invaded across the basement membrane and spread to the surrounding stromal tissue (Figure 1B, C). (Alkabban and Ferguson, 2024). In this stage, breast cancer can metastasize to other parts of the body by entering the bloodstream or through the lymphatic system (Nathanson et al., 2022). The prognosis of the patient is significantly affected by the extent of tumor progression. For instance, the 10-year overall survival rate of in situ -stage breast cancer is over 95%, while in non-metastatic but invasive breast cancer the 10-year overall survival rate is approximately 80%, and in metastatic breast cancer the 10-year overall survival rate is only 13% (Wang et al., 2017; Macià et al., 2012; Eng et al., 2016).

1.2.1 Breast cancer subtypes

Breast cancer is divided into four different subtypes based on immunohistochemical (IHC) evaluation; estrogen (ER) and progesterone (PR) receptor positive (ER+, PR+), human epidermal growth factor receptor positive (HER2+) and ER-, PR- and HER2-negative ie. triple-negative breast cancer (TNBC). ER and PR -positive breast cancers with low expression of the proliferation marker Ki-67 (<20%) are considered the luminal A subtype. Clinically these carcinomas have the best

prognosis because they are usually low grade, grow slowly and have a good treatment response to hormone therapy. ER-positive and/or PR-negative and HER2-negative breast cancers with high expression of Ki-67 (>20%) are considered the luminal B subtype. These carcinomas comprise 10–20% of luminal tumors and they have poorer prognosis because they grow faster compared to luminal A. TNBC comprise ~20% of all breast cancers. These tumors have an aggressive behaviour with high proliferation rate and are associated with poor prognosis (Orrantia-Borunda et al., 2022). Approximately 15-30% of breast cancers are HER2-positive. HER2 receptors are important for the mammary epithelial cells since they promote cell proliferation and differentiation (Rubin and Yarden, 2001). HER2 receptor amplification is shown to be significant factor in breast cancer pathogenesis and differentiation (Slamon et al., 1987). Slamon et al. (1987) showed that HER2-positive tumors have a more aggressive tumor phenotype, they tend to grow fast, and the prognosis of the patients is poor. Nevertheless, the prognosis of these patients has improved during the past years due to the development of HER2-targeted therapies.

1.2.2 Diagnosis & treatment strategies

Most of the patients, especially in the early stages of breast cancer, are asymptomatic and the tumors are discovered during mammography screening. When breast cancer progresses, it is often detected as a lump in the breast due to the desmoplastic reaction which means the increased collagen accumulation and crosslinking around tumor, resulting in a dense collagenous stroma (Walker, 2001). The current consensus regarding the treatment of localized (in situ) breast cancer is either breast-conserving surgery or mastectomy (total breast removal) for tumor removal, combined with postoperative radiation to ensure the elimination of all cancer cells. Very important factor regarding the surgical treatment of breast cancer is that the tumor is removed with sufficient margins of healthy tissue surrounding the tumor. This ensures that there is no tumor left in the breast after surgery. Currently, the margin should be at least 2 mm of healthy tissue surrounding the tumor (Morrow et al., 2016). Insufficient surgical margins have been shown to increase the risk of local recurrence in patients with DCIS (Dunne et al., 2009).

The treatment strategy of metastatic breast cancer is different. The purpose of the treatment is to slow down cancer progression, extend the patient's lifespan and improve the quality of life. The individual treatment plan is made considering the overall situation of the patient. In general, based on the patient's situation neoadjuvant treatment can be combined to chemotherapy before breast cancer surgery. More often, after the tumor removal patient gets adjuvant treatment which can be combined with chemotherapy (Wang and Wu, 2023). Endocrine therapy is part of the standard care

in cases of hormone receptor positive (ER+/PR+) metastatic breast cancer and can be utilized individually or in combination with chemotherapy. In case of HER2-positive breast cancer, anti-HER2-therapy is used such as trastuzumab or pertuzumab in combination with chemotherapy. (Leena Vehmanen, 2020). The current immune-oncological treatments that are intensifying the immune system to eliminate cancer cells are currently restricted to TNBC due to its rich density of immune cells in the tumor stroma (Loibl et al., 2024).

During the last decades the targeted therapy of breast cancer has improved dramatically. Trastuzumab (Herceptin®) was the first to revolutionize the targeted therapy of breast cancer in 1998 (Albanell and Baselga, 1999), when it was approved by US Food and Drug Administration (FDA) to treat breast cancer with HER2 amplification and still today trastuzumab in combination with chemotherapy is the cornerstone in the treatment of HER2-positive breast cancer (Loibl et al., 2024). Trastuzumab is a humanized monoclonal antibody that specifically binds to the outer domain of the HER2 receptor and prevents signalling cascades that intensify cell proliferation such as Ras-MAPK and phosphoinositide 3-kinase (PI3K-Akt) from being activated and, thus, prevents the proliferation of cancer cells (Nagata et al., 2004). Trastuzumab has also been shown to possess immunomodulatory properties through initiation of a phenomenon called antibody-dependent cellular cytotoxicity (ADCC). When trastuzumab binds to HER2 receptor on the surface of cancer cells, it helps the immune cells to recognize the malignant cells and eliminate them (Kute et al., 2012). The approval of trastuzumab has changed the treatment strategy of patients with HER2-positive breast cancer and extended their life expectancy remarkably (Slamon et al., 2001; Romond et al., 2005). However, majority of patients treated with trastuzumab develop resistance within a year. Multiple mechanisms mediate the development of trastuzumab resistance and it would be crucial to understand them better in order to develop novel therapeutics to improve the survival of patients with HER2-positive breast cancer. (Wang et al., 2022)

1.3 Ductal carcinoma in situ (DCIS)

DCIS is the most common non-invasive neoplasm accounting approximately 20% of breast cancers detected in mammography screenings (Ernster et al., 2002). In DCIS, the abnormal epithelial cells are confined within the basement membrane in the ducts and lobules without stromal invasion (Tomlinson-Hansen et al., 2023). While DCIS is generally indolent, patients still have an elevated risk for disease progression to invasive ductal carcinoma (IDC) and eventually approximately 25-60% of DCIS tumors will progress into IDC if left untreated (Wang et al., 2024).

The grade of the tumor predicts the tumor growth rate and patients' prognosis. There are three DCIS grades according to Scarff-Bloom-Richardson grading system, to describe the morphological features of the tumor. In grade I the appearance of cancer cells is mostly comparable to normal breast epithelial cells and the status is determined as "well differentiated". In grade II the cancer cells look less like the normal epithelial cells and have increased growth rate with status of "moderately differentiated". In grade III the cancer cells look very different compared to normal epithelial cells, and the status is "poorly differentiated". (Cserni and Sejben, 2020). Grade III DCIS seems to grow fast and possess higher potential to progress compared to low grade DCIS tumors (Cunha et al., 2010). The better the cancer cells are differentiated, the closer the cell morphology is to normal epithelial cell structure and, hence, these tumors typically are more benign.

Currently, DCIS management aims for the prevention of disease progression and local recurrence (Miligy et al., 2019). Currently, the consensus is that the optimal treatment for women with DCIS is the breast conserving surgery with clear surgical margins combined with radiation therapy. (Martínez-Pérez et al., 2017). According to the Finnish National Breast Cancer Diagnosis and Treatment Recommendation 2024, neither adjuvant nor neoadjuvant therapies are generally used in the treatment of DCIS in Finland. A special situation in which endocrine treatment can be considered is a hormone receptor-positive grade III DCIS in a patient under 50 years of age. It has been shown that in the treatment of DCIS, endocrine therapy such as tamoxifen reduces the risk of local recurrence but does not increase the patient's life expectancy (Cuzick et al., 2011; Wapnir et al., 2011). Nevertheless, treatment decisions are based on the characterization of the tumor, and they are always made individually according to the patients' overall situation.

1.3.1 DCIS tumor microenvironment

The focus of many current diagnostic and therapeutic strategies for breast cancer lies on the cancer cells that are proliferating and spearing. However, the interest in the tissue that surrounds the cancer cells, called tumor microenvironment (TME), has increased over the years. There is accumulating evidence showing that changes in the TME affect both tumor initiation and progression (Gibson et al., 2023). The significance of the TME in DCIS progression into IDC is supported by the fact that genetic changes in the epithelial cells are similar between DCIS and IDC (Casasent et al., 2018), suggesting that the role of the TME and phenotypic plasticity of the cancer cells might be bigger in DCIS progression than the emergence of new invasion promoting mutations. There is a growing body of evidence demonstrating that cancer cells and the TME communicate closely and, therefore,

it is necessary to understand the changes in the TME during cancer development and progression and define their links to clinical outcomes.

1.3.1.1 Myoepithelial cells

Myoepithelial cell layer is located between the luminal epithelial cells and the basement membrane. Multiple studies have shown that in addition to their contractile properties in milk ejection, myoepithelial cells seem to contribute the proliferation, differentiation, and polarity of the luminal epithelial cells. In addition, myoepithelial cells contribute to the synthesis of the basement membrane by expressing laminins and collagen IV. (Gudjonsson et al., 2005). It has also been shown that in breast cancer myoepithelial cells form a dynamic barrier restricting cancerous luminal cells to escape (Sirka et al., 2018). The presence or loss of myoepithelial cells is a very significant factor affecting the diagnosis of breast cancer patients. The loss of myoepithelial cells around the cancer lesion indicates the presence of invasion in breast cancer. The mechanisms of how myoepithelial cells modulate breast cancer progression from DCIS to IDC remain poorly defined. However, there is accumulating evidence that in DCIS myoepithelial cells can facilitate tumor progression for instance by up-regulating certain proteins that promote tumor invasion such as glycoprotein tenascin C (TN-C) isoforms (Adams et al., 2002).

1.3.1.2 Immune cells

Immune cells are a significant part of the TME in breast cancer (Goff and Danforth, 2021). When the normal mammary epithelial cells become malignant, the membrane proteins of the cells are altered, and the immune system is recognizing the abnormal cells trying to kill them. The theory of immune cells recognizing tumor cell neo-antigens and causing an anti-tumor reaction against neoplastic cells was first represented by Sir Frank Mac Farlane Burnet in 1950-1970 (Burnet, 1964; Burnet, 1971). The immune cells in the tumor stroma (called as immune cell infiltration) consists of innate immune cells including macrophages, natural killer cells (NK) and dendritic cells (DC) and adaptive immune cells consisting of B cells and T cells (Li et al., 2022).

It has been shown that the amount of immune cells, both innate and adaptive, increases in DCIS and IDC compared to normal breast tissue (Gil Del Alcazar et al., 2017). However, breast cancer is not a very immunogenic cancer compared to other cancer types, such as melanoma, but it has been shown that a subset of breast cancers have a rich immunogenic TME such as TNBC (Stanton et al., 2016). Further, it has been noticed that the immune cells play a critical role in the progression and therapeutic response of breast cancer. For instance, high levels of tumor infiltrating lymphocytes

(TILs) are associated with good prognosis in invasive HER2-positive breast cancer. TILs also contribute to a beneficial response to anti-HER2 antibody trastuzumab because of the ability of trastuzumab to induce the immune response against cancer cells (Joensuu et al., 2009). However, it is less clear what is the effect of TILs in DCIS progression and what is their relevance to breast cancer prognosis (Pruneri et al., 2017). However, it was found that the presence of macrophages in DCIS was found to have prognostic relevance. Campbell et al. (2017) perceived higher levels of CD68+ macrophages in high grade DCIS compared to low grade DCIS (Campbell et al., 2017), and Chen et al. (2020) showed that greater density of CD68+ macrophages is associated with worse prognosis in DCIS patients (Chen et al., 2020). The cancer cells themselves also have the ability to manipulate the immune system in many ways to avoid the anti-tumor responses (Gibson et al., 2023). For instance, cancer cells can modify the TME to become more immunosuppressive and tumor promoting together with other cells of the TME, ultimately leading to tumor progression and immune evasion. These mechanisms are targeted by immune-oncological therapies.

1.3.1.3 Angiogenesis

The new growth of blood vessels from the pre-existing vessels is called angiogenesis. Angiogenesis is a phenomenon which occurs in both healthy and disease state when requirements for blood supple to the tissue are altered. Angiogenesis promotes tumor growth, progression and metastasis, and cancer cells and the TME contribute to angiogenesis by sending proangiogenic factors that allow the development of new blood vessels (Ayoub et al., 2022). For instance, vascular endothelial growth factor (VEGF) released by the cancer cells promotes the proliferation of endothelial cells that form the new vessels. In cancer, sustained proliferation of malignant cells increases the need for more blood supply (Weis and Cheresh, 2011). In addition, in solid tumors like breast cancer, oxygen and nutrient levels gradually decrease in the tumor core, and the deficiency of oxygen causes hypoxia, which contributes to vascular remodelling (Bottaro and Liotta, 2003). The resulting new vessel network is typically leaky and not very stable but often stable enough to help the cancer cells grow and metastasize (Weis and Cheresh, 2005). In general, it has been shown that increased density of micro vessels due to angiogenesis in breast cancer TME is associated with decreased survival (Gibson et al., 2023). In DCIS, it has been suggested that increased periductal vessel formation is associated with local invasion (Teo et al., 2003). However, there are conflicting results on this showing that pure DCIS display more pro-angiogenic factor compared to DCIS with coexisting invasion (Wülfing et al., 2005).

1.3.1.4 Extracellular matrix (ECM)

ECM is a complex molecular network with biomechanical and biochemical properties. The mammary gland ECM, including the basement membrane, is composed of many different proteins that maintain its structure such as collagens, fibronectin, and laminins (Allinen et al., 2004). Overall, the ECM is an important factor in cell and tissue homeostasis. In breast cancer, changes in the ECM expression levels and remodelling are driven by cancer cells or cancer-associated fibroblasts (CAFs), and promote cancer progression (Lepucki et al., 2022). CAFs can cause the ECM to become more fibrous which can be seen as a desmoplastic reaction around tumor structures (Insua-Rodríguez and Oskarsson, 2016). The increased expression of fibrillar collagens, fibronectin (fibril-forming glycoprotein) and other ECM proteins contributes to the increased stiffness of the TME. Furthermore, it has been shown that stiff TME promotes breast cancer progression (Papanicolaou et al., 2022). When DCIS develops into IDC, the disruption of basement membrane allows cancer cells to invade to the surrounding tissue either as a stream or in single cells (Clark and Vignjevic, 2015). To be able to understand the mechanism behind this phenomenon would allow us to find solutions to prevent the cancer invasion.

1.3.2 Challenges with clinical management of DCIS

DCIS encompasses a heterogeneous group of tumors that differ in terms of morphology, molecular features, clinical manifestation, and the probability to advance into IDC. DCIS, if appropriately managed, is a tumor with very low-risk but some DCIS tumors have more aggressive and malignant features (Martínez-Pérez et al., 2017). While aggressive DCIS cases only account for a small proportion of all DCIS cases, all patients with DCIS diagnosis receive roughly the same treatments. In this respect, the main challenge in the clinical management is to avoid the over-treatment of “low- risk” DCIS lesions sparing patients with good prognosis from radical surgery while avoiding under-treatment of “high-risk” lesions in order to minimize the risk of recurrence or progression into IDC. Currently, determining which non-invasive DCIS lesions will develop into IDC (if left untreated) or predicting the risk of metastatic recurrence in DCIS associated with invasion is still inadequate and, therefore, the clinical management of DCIS as well as optimization of the treatment decisions are challenging (Martínez-Pérez et al., 2017). Therefore, more accurate and efficient prognostic and predictive biomarkers are needed to guide the decisions regarding the therapy options to improve the clinical management of DCIS lesions.

1.3.3 Neoductgenesis

A theory of a new, poorly understood subtype of breast cancer called neoductgenesis was suggested already twenty years ago (Tabar et al., 2004). According to mammographic screening, Tabár and colleagues identified tumors associated with a large number of abnormally packed “casting type” calcifications that were pointing in different directions. Based on these findings, they noticed that this breast cancer subtype forms duct-like structures which are filled with cancerous cells and these diffusely infiltrating malignant cells were spreading generating a large tumor burden. Hence, they proposed that this duct-forming process represents a special type of neoplasia that neither fits in any classical group of invasive nor in situ breast cancer. Therefore, they proposed the name ductal adenocarcinoma of the breast (DAB) to facilitate the description of this malignancy with neoductgenesis as a distinct breast cancer subtype. (Tabár et al., 2022).

According to pathology experts, roughly 10% of patient with high grade DCIS diagnosis exhibit signs of neoductgenesis. Neoducts are thought to originate from the major lactiferous ducts which then branch into smaller ducts (Tabár et al., 2022). These duct-like structures propagate by producing numerous side branches which are tightly packed and filled with cancer cells without a normal organized structure and lacking TDLUs. Tabár et al. (2022) suggested that the formation of these newly formed duct-like structures resulting from neoductgenesis is driven by stem cells (Tabár et al., 2022). However, the underlying mechanisms behind this new duct formation are poorly understood.

1.3.3.1 Histopathological features of neoductgenesis

The histopathological features of neoductgenesis have been previously described mostly by Tabár et al. (2022). First of all, neoducts were shown to be distinct compared to normal breast epithelial ducts in thick histopathology samples, as neoducts are much larger in size compared to the thin structures of normal breast ducts and TDLUs (Tabár et al., 2022). Nevertheless, it has been shown that basement membrane surrounding the neoducts is intact. In addition, a robust desmoplastic reaction has been detected around these duct-like structures and suggested to be linked to epithelial-to-mesenchymal transition (EMT). Thick lymphocytic infiltration in stroma and the overexpression of TN-C around neoducts were also shown to be typical around the neoduts (Tabár et al., 2022). TN-C is a ECM glycoprotein expressed during fatal and pubertal mammary gland development (Jahkola et al., 1998). It has also been shown that TN-C is a promotor of cell migration and survival as well as angiogenesis in cancer. Overexpression of TN-C correlates with poor prognosis in breast cancer patients and it contributes to formation of the metastatic niche in breast cancer (Oskarsson et

al., 2011). In addition, high grade of the tumor and high proliferation index have been associated with neoductgenesis (Zhou et al., 2017). According to Zhou et al. (2014) HER2 receptor overexpression seems to be strongly present in the neoducts as well (Zhou et al., 2014).

1.3.3.2 The impact of neoductgenesis to the management of breast cancer

Several studies have found that neoductgenesis is associated with more aggressive tumors (Łazarczyk et al., 2023; Zhou et al., 2014; Zhou et al., 2017; Tabár et al., 2022). For instance, the overexpression of HER2 receptor, also prominent in neodcuts, is associated with more aggressive tumor phenotype (Loibl and Gianni, 2017). In addition, the abundant and abnormally packed casting-type calcifications and overexpression of TN-C glycoprotein in patients neoductgenesis support the aggressive tumor phenotype of neoductgenesis (Wawrzyniak et al., 2020). Follow up of breast cancer patients with signs of neoductgenesis revealed poorer survival of these women suggesting that neoductgenesis could be linked to the malignant and often fatal nature of these tumors (Tabár et al., 2022). Currently, breast cancer with features of neoductgenesis is diagnosed as DCIS because the duct-like tumor structures are surrounded by a myoepithelial cell and an intact basement membrane which are currently considered essential criteria for carcinoma in situ diagnosis. The current diagnosis of these lesions as DCIS is likely to mislead the estimated prognosis of these patients because DCIS is associated with very good prognosis. Importantly, DCIS diagnosis can have negative impact on the treatment decisions because adjuvant therapy in these cases might be beneficial. Currently, patients with non-invasive breast cancer associated with neoductgenesis do not have the opportunity to get HER2-targeted therapy because it is currently not used for the treatment of HER2-positive DCIS due to the lack of proof of its significant therapeutic effect (Cobleigh et al., 2021), although these patients might get benefit from it.

Breast conserving surgery might not be a good option for patients with neoductgenesis because the neoducts often expand from the nipple towards the chest wall and the real extent of the cancer lesion is larger than what can be seen in mammograms based on calcifications. This is a caused by newly formed, uncalcified extensions of the neoducts, making the surgical management even more difficult (Tabár et al., 2022). Therefore, multimodal imaging including MRI could be helpful for the assessment of the full extent of the tumor, and whether breast-conserving surgery is possible. Otherwise, the breast-conserving surgery might leave actively growing part of the cancer in the breast. Because of these challenges, it would be essential to recognize the invasive behaviour and the true tumor burden of neoductgenesis in breast cancer so that the patients could be correctly diagnosed and treated according to their actual needs. In order to improve the diagnostics and

treatment of women with breast cancer associated with neoductgenesis, it is essential to differentiate the neoducts from DCIS and to understand the molecular features that are specific to neoductgenesis. With correct information, the pathologists could recognize these cases, and give the patient an accurate diagnosis with proper treatment.

1.4 Aims of this Master's thesis

This master's thesis aims to provide increased knowledge and histopathological markers for neoductgenesis to ultimately improve the current DCIS diagnostics. To this end, imaging mass cytometry (IMC), immunohistochemistry (IHC) and immunofluorescence (IF) staining will be used to distinguish the spatial molecular features of selected breast cancer tissue samples that a pathologist has evaluated as high grade DCIS cases with or without neoductgenesis. In addition, the efficacy of a novel HER2-targeted therapy will be investigated in vitro.

As high grade DCIS and tumors with neoductgenesis are typically associated with immune cell infiltration observed in histopathology, Hyperion IMC provides the means to characterize and compare the immune cell profiles and other markers of interest between DCIS samples with and without neoductgenesis to identify potential differences broadly and quantitatively. The expression level and localization of proteins associated with HER2 signalling, myoepithelial features, vascularization, and ECM composition in neoductgenesis can also be evaluated by IF. Together, these approaches are expected to reveal tissue and molecular level features that are specific to neoductgenesis and can be further exploited in the development of diagnostics and treatment of DCIS. The primary goal of this MSc thesis is to detect differential structural and molecular features between conventional DCIS and DCIS associated with neoductgenesis. Furthermore, this thesis aims to provide novel insight in the invasive nature of neoductgenesis, and possibly also candidates for novel biomarkers to improve the current diagnostics of patients with breast cancer associated with neoductgenesis.

Patients with neoductgenesis could benefit from HER2-targeted therapies. In this MSc thesis, the efficacy of disulfide bridge-stabilized single-chain variable fragments (ds-scFv-Fc) derived from trastuzumab will be compared to the current trastuzumab used in clinic (Herceptin). The capacity of these therapeutic antibodies to inhibit the proliferation of HER2-positive breast cancer cells will be analysed to evaluate whether the ds-scFv-Fc antibody fragments with improved pharmacological properties have equal or even better ability compared to trastuzumab (Herceptin). Many patients with HER2-positive breast cancer eventually develop resistance against trastuzumab and, hence, the unmet need to develop new strategies to overcome the resistance mechanisms is acute.

With diagnostic biomarkers specific to neoductgenesis, the pathologists could recognize these cases to mitigate the challenges in the clinical management of DCIS: over-treatment of “low risk” DCIS lesions and under-treatment of “high-risk” lesions. Distinguishing the patients with neoductgenesis early could improve the prognosis of these patients. This study calls for attention to this fatal subtype of breast cancer that is currently underdiagnosed as in situ carcinoma. By utilizing state-of-the-art molecular profiling technologies, this study aims to gain the evidence to support the distinct nature of neoductgenesis as well as to provide much needed histopathological markers for the improvement of the current diagnostics of breast cancer with neoductgenesis.

2 Results

2.1 High grade DCIS tumors with neoductgenesis exhibit specific histopathological features

The patients sample panel utilized in the study consists of formalin-fixed and paraffin-embedded (FFPE) tissue samples of high grade DCIS tumors evaluated by a pathologist: three tumor samples representing conventional DCIS (ID301, ID302, ID305) and three tumor samples representing DCIS with neoductgenesis (ID401, ID403, ID405). Detailed description of patient samples in materials and methods section in page 43 (Table 1). H&E-stained tissue sections of all DCIS tumor samples showed typical features of high grade DCIS, and the samples with neoductgenesis showed the cancerous duct-like structures and dense collagenous stroma (desmoplastic reaction) that have been associated with neoductgenesis (Figure 2).

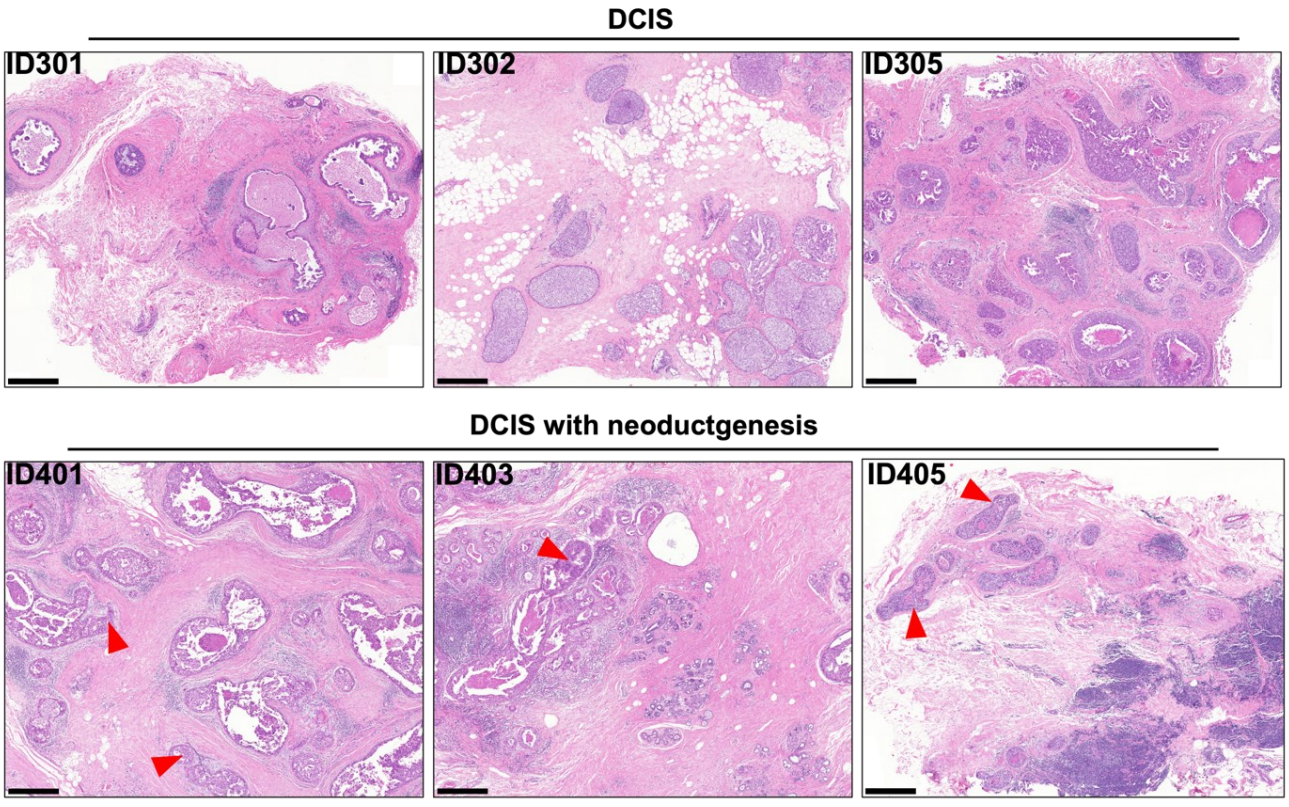

Figure 2. High grade DCIS tissue with signs of neoductgenesis exhibits closely packed and contorted, newly formed ducts. H&E staining of patient samples used in this study: three tumor samples representing DCIS (ID301, ID302, ID305) and three tumor samples representing DCIS with signs of neoductgenesis (ID401, ID403, ID405). H&E staining of DCIS with neoductgenesis shows the duct-like structures representing neoductgenesis (red arrowheads). Scale bars: 500 μm.

2.1.1 High grade DCIS tumors with neoductgenesis show abundant stromal immune cell infiltration

High grade DCIS is typically associated with immune cell infiltration in histopathology. Based on the H&E staining of the tumor samples used in this study, stromal immune cell infiltration was observed in a few spots in two of the DCIS tumor samples ID301 and ID305, and abundant stromal immune cell infiltration was observed in all three neoductgenesis tumor samples (Figure 3). In addition, in neoductgenesis samples, immune cell infiltration was associated with the cancerous duct-like structures (Figure 3).

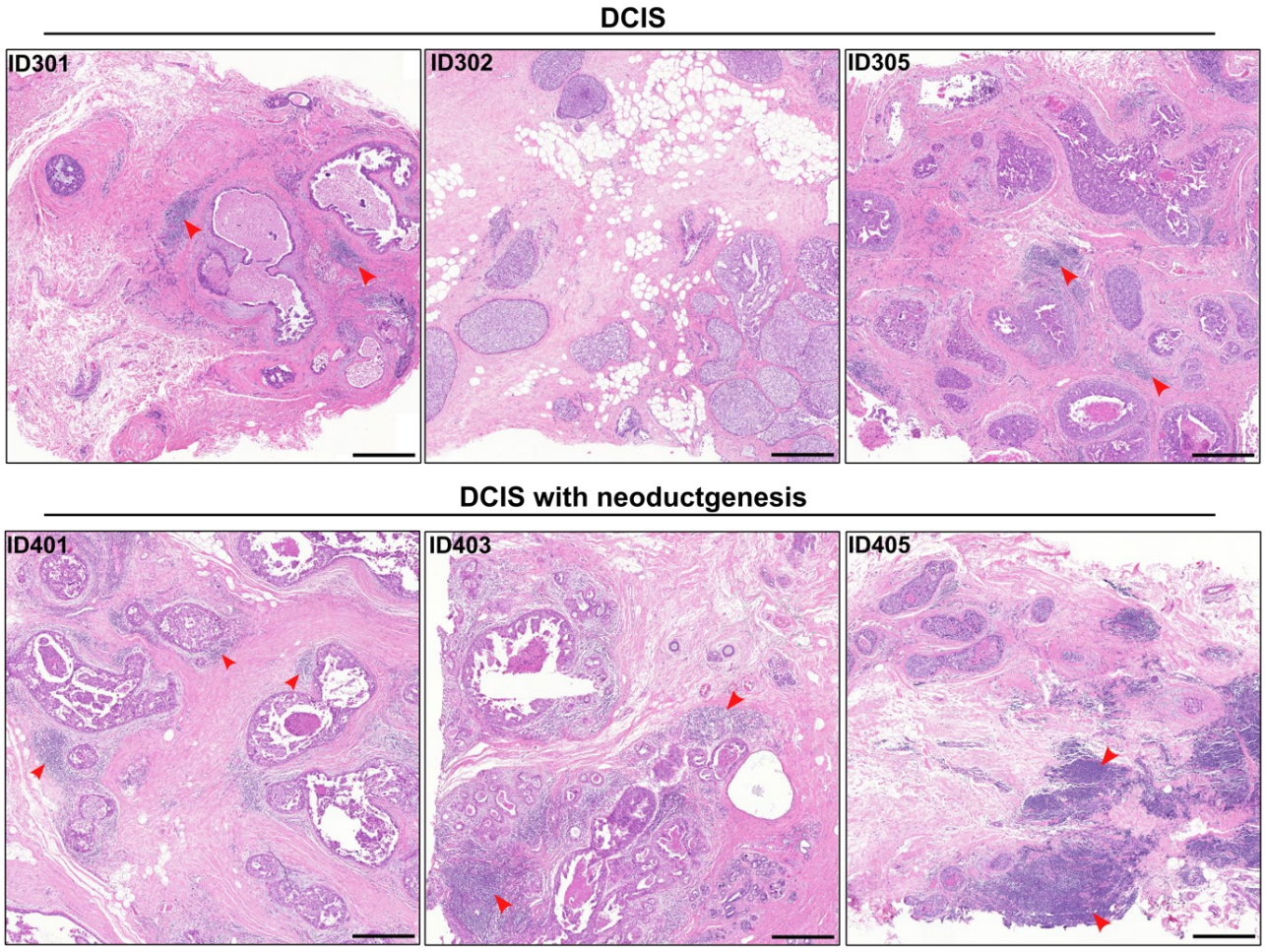

Figure 3. High grade DCIS tissues with the signs of neoductgenesis exhibits strong stromal immune cell infiltration. H&E staining of DCIS tissues with or without signs of neoductgenesis shows abundant immune cell infiltration. Immune cell infiltrates marked with red arrow heads. Scale bars: 500μm.

2.1.2 High grade DCIS tumors with neoductgenesis show overexpression of HER2 receptor

Previous studies have shown that tumor structures resulting from neoductgenesis are usually HER2-positive (Tabár et al., 2022; Zhou et al., 2014). IHC staining of HER2 was utilized to determine the HER2 receptor status in the DCIS tumor samples with and without neoductgenesis (Figure 4). Overall, the expression level of the HER2 receptor was variable between the samples. DCIS tumor samples with neoductgenesis (ID401 and ID403) showed strong HER2 receptor overexpression (Figure 4). ID405 seemed to be HER2-positive as well but the tissue section was of poor quality and not representative. Two of the DCIS tumor samples (ID305 and ID301) also showed strong HER2 receptor expression, but the third one (ID302) appeared HER2-negative (Figure 4).

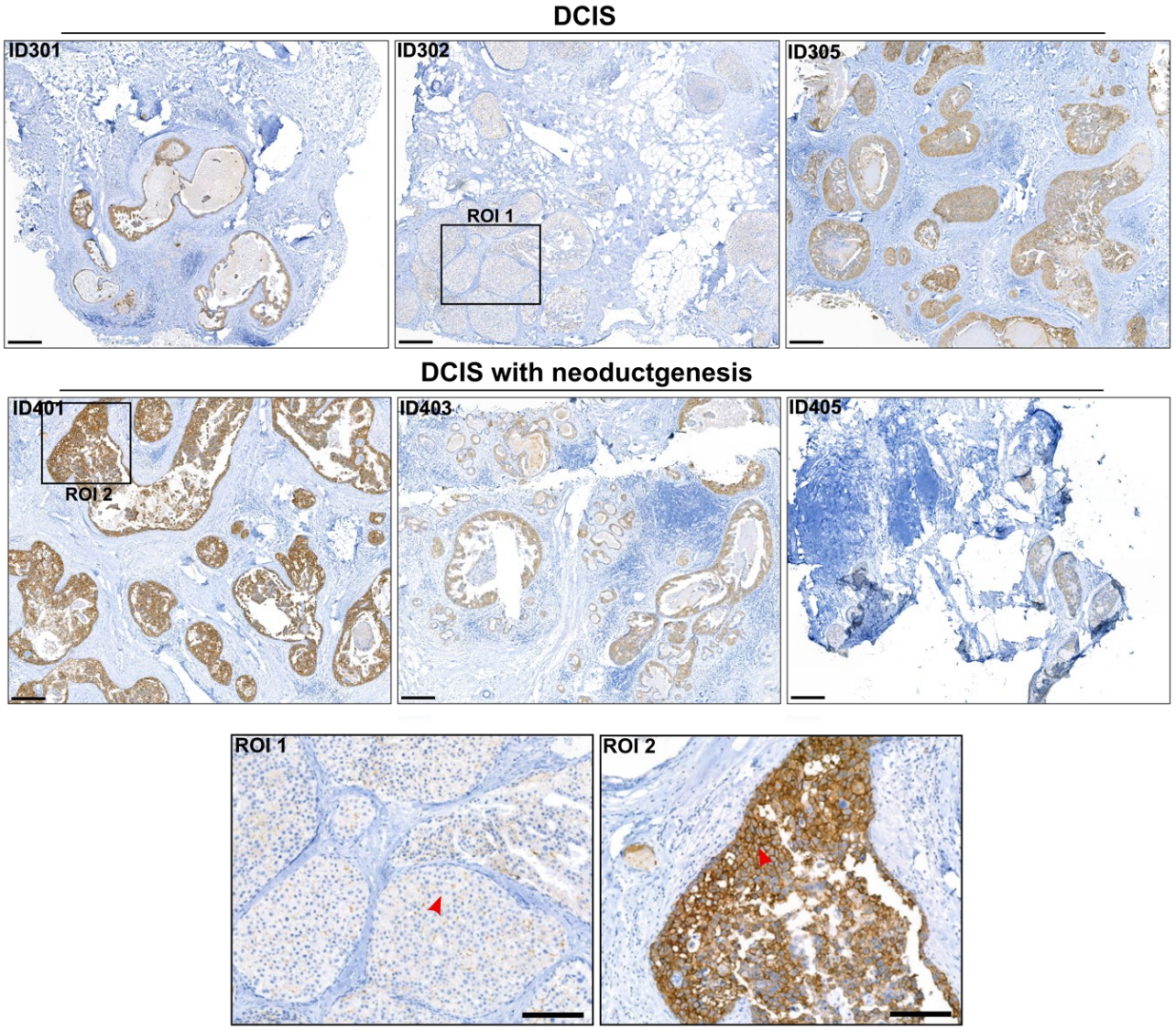

Figure 4. IHC staining of HER2 receptors in DCIS tumor samples with and without neoductgenesis. The expression level of the HER2 receptor (brown) in the tumor samples is variable. DCIS tumor sample

ID305 as well as DCIS tumor sample with neoductgenesis ID401 show strong HER2 receptor expression in the surface of tumor cells (ROI 2). HER2 receptor amplification is not seen in the ID302 sample (ROI 1). Red arrowheads are pointing to the HER2 receptor expression in cancer cells. Scale bars: 200μm and 100μm in ROIs.

2.2 IMC analysis of high grade DCIS tumors reveals that neoductgenesis is associated with differences in several cell types

The Hyperion IMC analysis was utilized for the broad characterization of the high grade DCIS tumor samples with and without neoductgenesis. Initially, tissue sections were stained using an antibody panel containing 28 metal-labelled antibodies. Two different regions of interest (ROIs) per tissue (maximum 1 mm x 1mm) were selected for the IMC laser ablation (Figure 5). After laser beam ablation, the ablated material is automatically transferred to mass cytometer for the time-of-flight detection of the metal ions from each ionized metal tag.

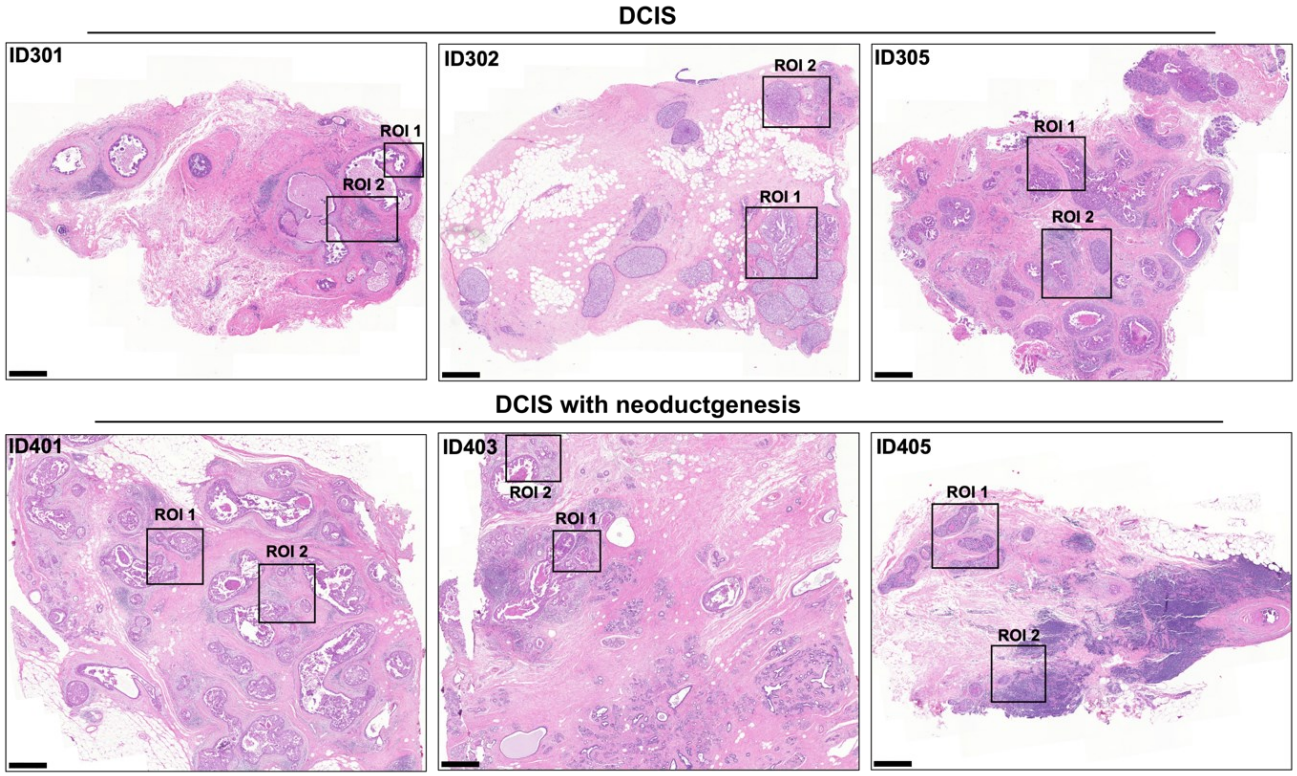

Figure 5. Two different ROI areas were selected per tumor tissue for IMC. Representative 1 mm x 1 mm areas of tissue were selected in H&E-stained tumor sections. Scale bars: 500μm.

As expected, the presence of α smooth muscle actin (αSMA) surrounding the tumors in both ROI areas indicates that the myoepithelial cell layer is present (Figure 6A, B). Strong immune cell infiltrates indicated by the leukocyte marker CD45 were more prominent in neoductgenesis samples

and localized particularly around the distorted duct-like structures (Figure 6A, B). In DCIS tumor samples the immune cells infiltrates were observed to be further away from the tumor acini. According to the IMC results, the presence of macrophages (CD68) was increased in the stroma of neoductgenesis tumor samples compared to DCIS tumor samples (Figure 6A, B). However, DCIS tumors seemed to have more intratumoral macrophages compared to neoductgenesis tumors, although stromal macrophages were more prominent in the latter tumor group. In addition, neoductgenesis tumor samples showed increased presence of stromal intermediate filament vimentin (VIM) -positive stromal cells as well as increased density of blood endothelial cells (CD31) (Figure 6A, B). DCIS tissues with neoductgenesis showed also elevated level of Ki67, a marker for cell proliferation (Figure 6A, B).

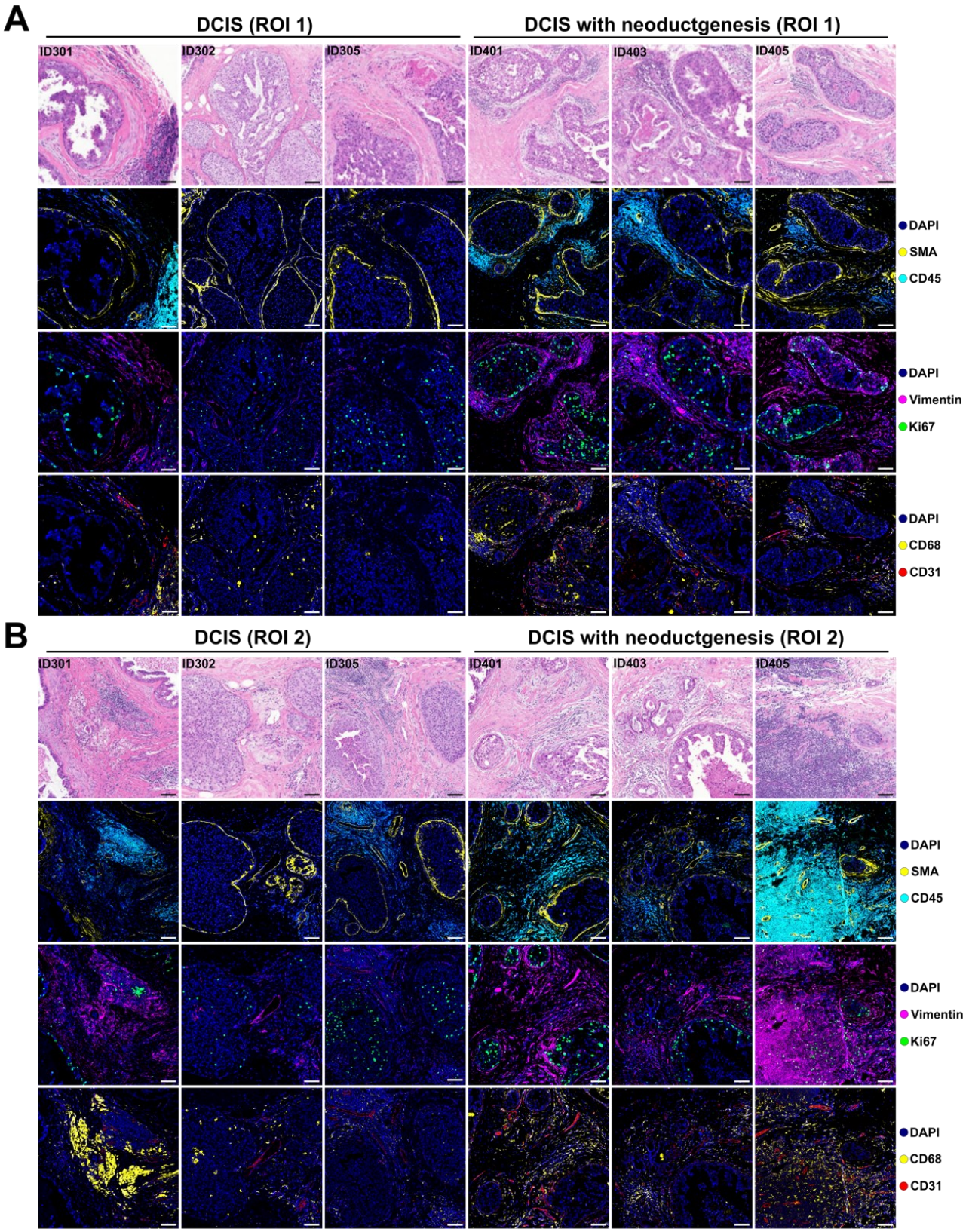

Figure 6. Representative results of the IMC analysis of DCIS tumor samples with and without neoductgenesis. The IMC data from two ROIs demonstrates that DCIS tumor samples with and without neoductgenesis exhibit a myoepithelial cell layer (alpha smooth muscle actin, αSMA) surrounding the tumor structures. Neoductgenesis tumor samples show an increase in stromal vimentin levels, vascularization (blood endothelium, CD31), cancer cell proliferation (Ki67) and stromal macrophages (CD68). In addition, in

neoductgenesis tumor samples, immune cell infiltration (leukocytes, CD45) is prominent. Scale bars: 100 μm.

2.3 Validation of IMC results by IF

2.3.1 Stromal vascularity is higher in DCIS tumors with neoductgenesis

Based on the IMC data, the IF staining of high grade DCIS tumors with and without neoductgenesis were conducted to validate the forementioned findings in a larger tissue area. Five different markers, CD68, CD31, VIM, Ki67 and CD45, were selected for validation based on their differential occurrence in DCIS and neoductgenesis tumor samples to indicate stromal/intratumoral macrophages, vascularity, vimentin levels, cell proliferation and total leukocytes, respectively. In the validation cohort, FFPE tissue sections from seven different patients were utilized; four DCIS tumor samples and three neoductgenesis tumor samples, some of which were from the same samples already used for IMC. Detailed description of patient samples in materials and methods section in page 43 (Table 1). Samples were stained with primary antibodies against CD31, VIM, Ki67, CD68 and CD45 and imaged by confocal microscopy taking 2-4 large images per each sample from different parts of the tissue area, depending on the size of the tissue section. The resulting fields of views (FOVs) were quantified for the signal intensity of Ki67, CD31, CD68, and VIM. CD45 marker was left unquantified because the staining was not successful. In the image analysis, tumor and stroma were distinguished with epithelial cell marker keratin 8 (KRT8) (Figure 7A, 8A, 9A). The KRT8-positive tumor areas were excluded from the quantification of the stromal signals. The area of intratumoral Ki67 was quantified exclusively in the tumor area and normalized to the relative area of nuclei (DAPI).

According to the results of IF, DCIS tissues with neoductgenesis showed significantly higher vascularization (CD31 + area) in tumor stroma ($p=0.0002$) compared to high grade DCIS tumor samples without neoductgenesis (Figure 7). Tumor samples with neoductgenesis also showed elevated stromal vimentin levels but this difference did not reach statistical significance ($p=0.1194$) (Figure 8). Interestingly, the same level or even more proliferation (Ki67 positive cells) were seen in DCIS tumors without neoductgenesis, but this result was not statistically significant ($p=0.1559$) (Figure 9). In any case, the elevated cell proliferation observed in IMC analysis (Figure 6) could not be observed in the analysis of larger tumor areas (Figure 9).

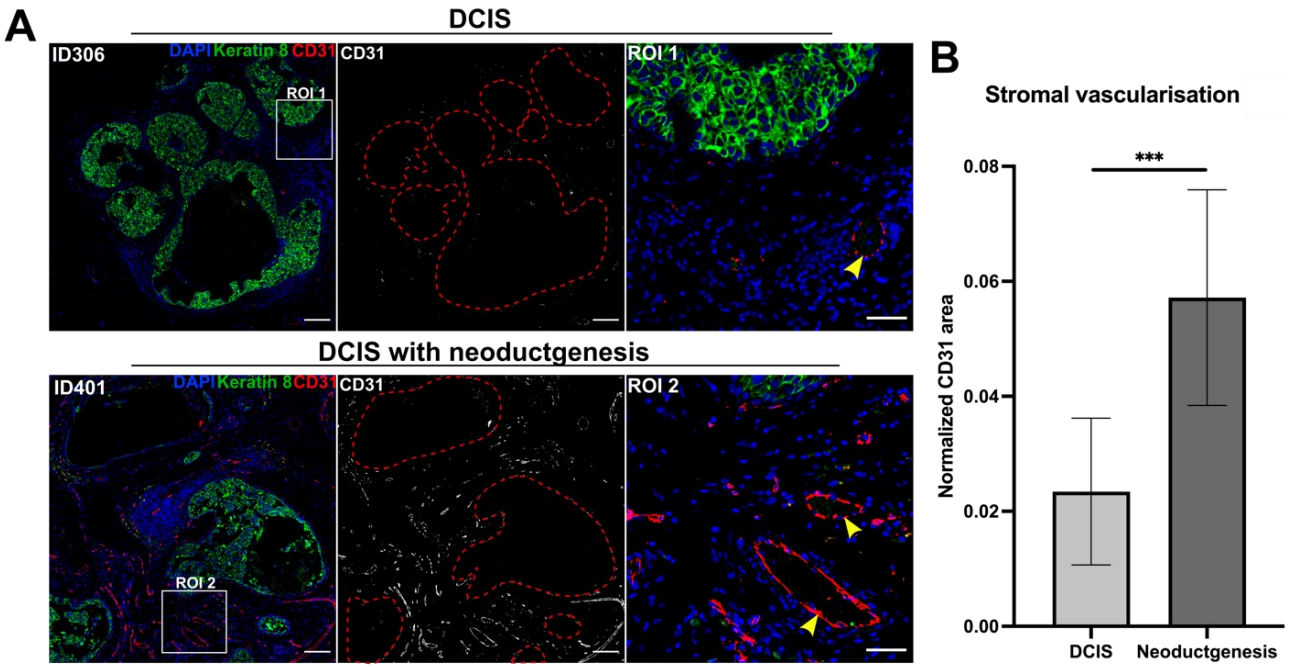

Figure 7. High grade DCIS with neoductgenesis exhibits significantly increased stromal vascularisation. Representative IF images of the vascular endothelial cell marker CD31 (red) (A), and quantification of the CD31 signal area normalized to total area of the stroma (B) [mean ± SD, n(DCIS) = 10 FOVs from 4 patients, n(DCIS with neoductgenesis) = 11 FOVs from 3 patients]. Tumor and stroma were separated with the use of KRT8 (green; tumor border indicated with dashed lines). Nuclei were labelled with DAPI. Yellow arrowheads point to vascular endothelial cells (A). Neoductgenesis tumor samples exhibit significantly higher presence of blood vessels in the tumor stroma compared to conventional DCIS tumors (p=0.0002, two-tailed Student's t-test) (B). Scale bars: 150 μm and 50 μm in ROIs.

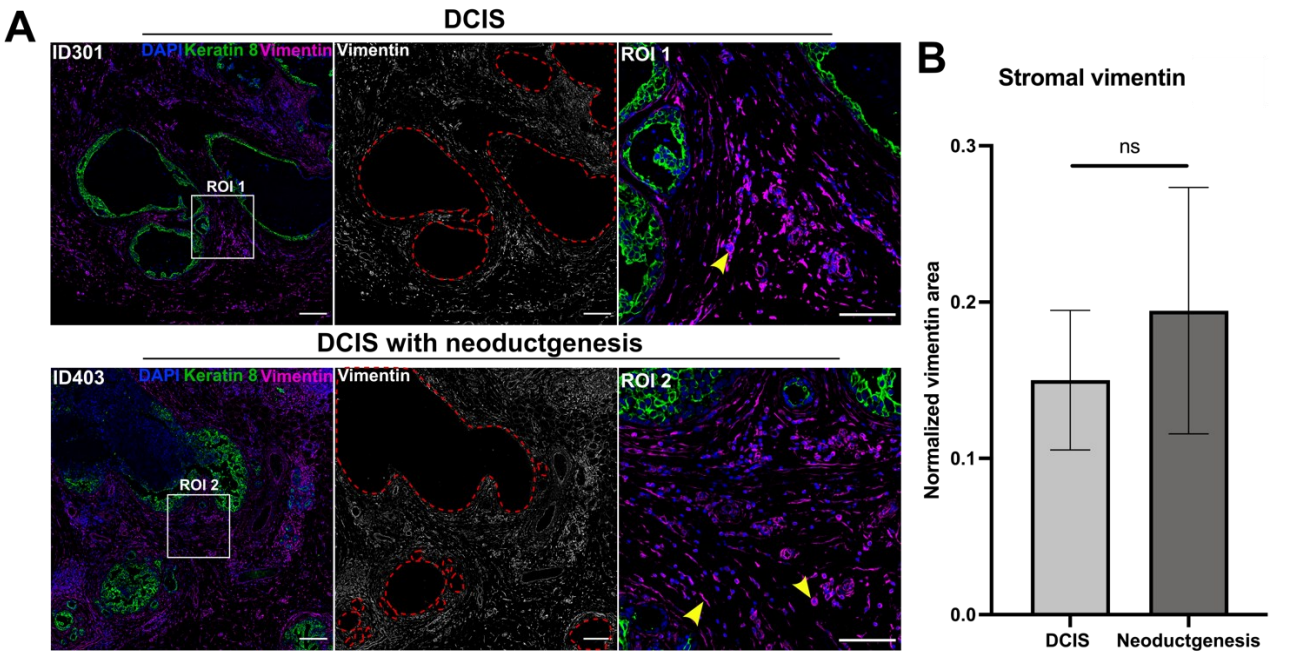

Figure 8. High grade DCIS tumors with neoductgenesis show no statistically significant difference in stromal vimentin. Representative IF images of the intermediate filament vimentin (magenta) (A), and quantification of the vimentin signal area normalized to total area of the stroma (B) [mean ± SD, n(DCIS) = 12 FOVs from 4 patients, n(DCIS with neoductgenesis) = 11 FOVs from 3 patients]. Tumor and stroma were separated with the use of KRT8 (green; tumor border indicated with dashed lines). Nuclei were labelled with DAPI. Yellow arrowheads point to vimentin-positive stromal cells (A). Neoductgenesis tumor samples exhibit

higher levels of vimentin in the tumor stroma compared to conventional DCIS tumors, but not statistically significantly (p=0.1194, two-tailed Student's t-test) (B). Scale bars: 200 μm and 100 μm in ROIs.

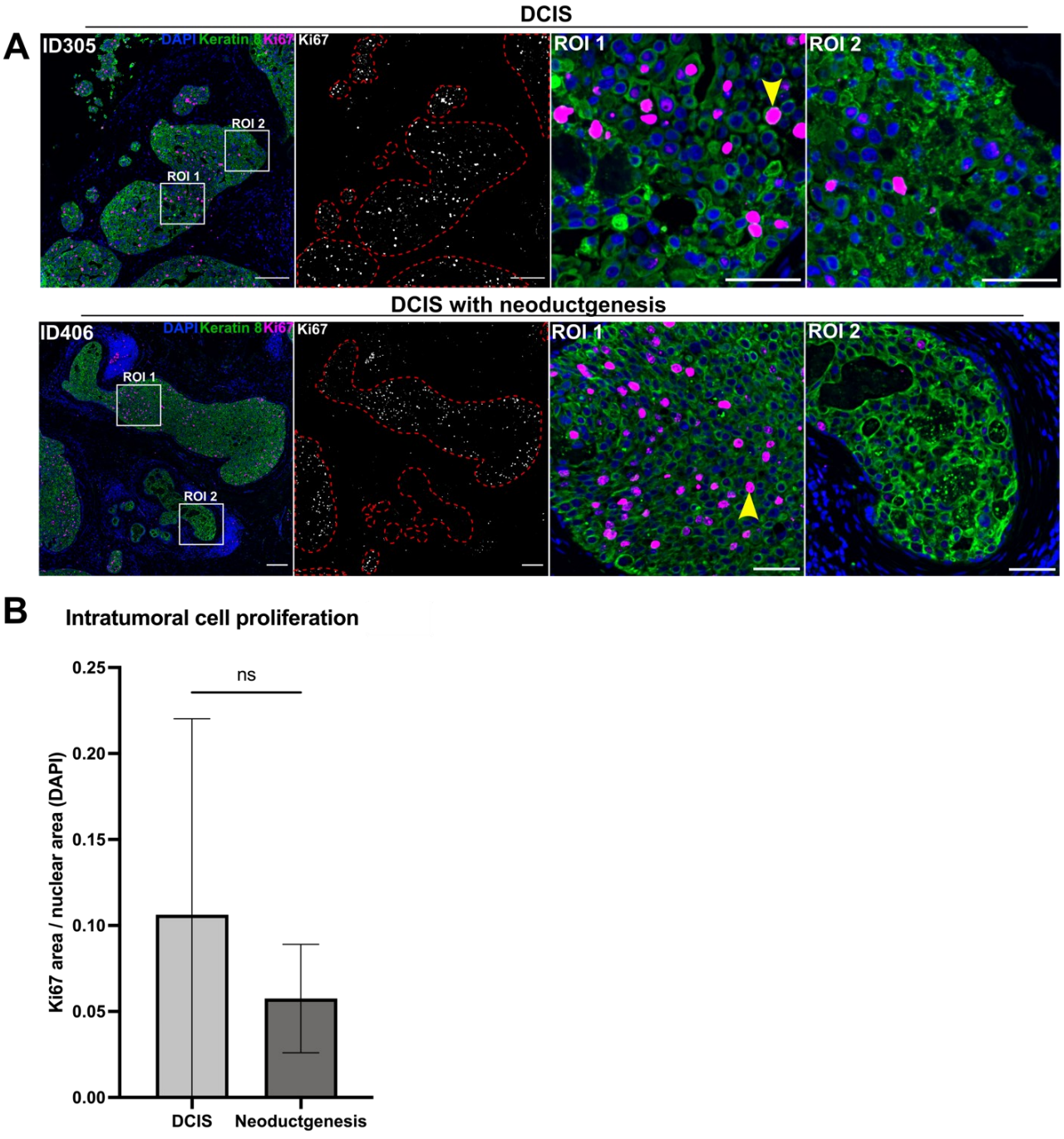

Figure 9. High grade DCIS tumors with neoductgenesis show no statistically significant difference in cancer cell proliferation. Representative IF images of the cell proliferation marker Ki67 (magenta) (A), and quantification of the intratumoral Ki67 area in the tumor areas and normalized to the relative area of nuclei (DAPI) (B) [mean ± SD, n(DCIS) = 12 FOVs from 4 patients, n(DCIS with neoductgenesis) = 11 FOVs from 3 patients]. Tumor and stroma were separated with the use of KRT8 (green; tumor border indicated with dashed lines). Yellow arrowheads point to Ki67-positive cells (A). Neoductgenesis tumor samples exhibit less cancer cells proliferation compared to conventional DCIS tumors, but not statistically significantly (p=0.1559, Mann-Whitney U-test) (B). Scale bars: 150 μm and 50 μm in ROIs.

2.3.2 The amount of intratumoral macrophages is reduced in DCIS tumors with neoductgenesis

Based on the IMC data, an abundance of intratumoral macrophages were observed particularly in DCIS tumor samples without neoductgenesis (n=3), especially in ID302 that was the only HER2 negative tumor in the cohort. Hence, CD68 IF staining of DCIS tissues with and without neoductgenesis (n=3-4) were utilized to validate the finding using more tumor samples and larger tissue areas. Three to four large images from different parts of the tissue area were imaged using confocal microscopy (Figure 10A) and quantified by image analysis (Figure 10B, C). In the image analysis, tumor and stroma were distinguished with the use of KRT8, and the area of CD68+ cells inside (Figure 10B) and outside (Figure 10C) of the tumor tissue was quantified and normalized to the relative tumor area and stromal area, respectively. The analysis shows a significantly higher amount of intratumoral macrophages in DCIS samples compared to DCIS tissue samples with features of neoductgenesis ($p=0.0001$) (Figure 10B). In turn, no statistically significant difference was seen in the amount of stromal macrophages between the tumor groups ($p=0.1100$) (Figure 10C).

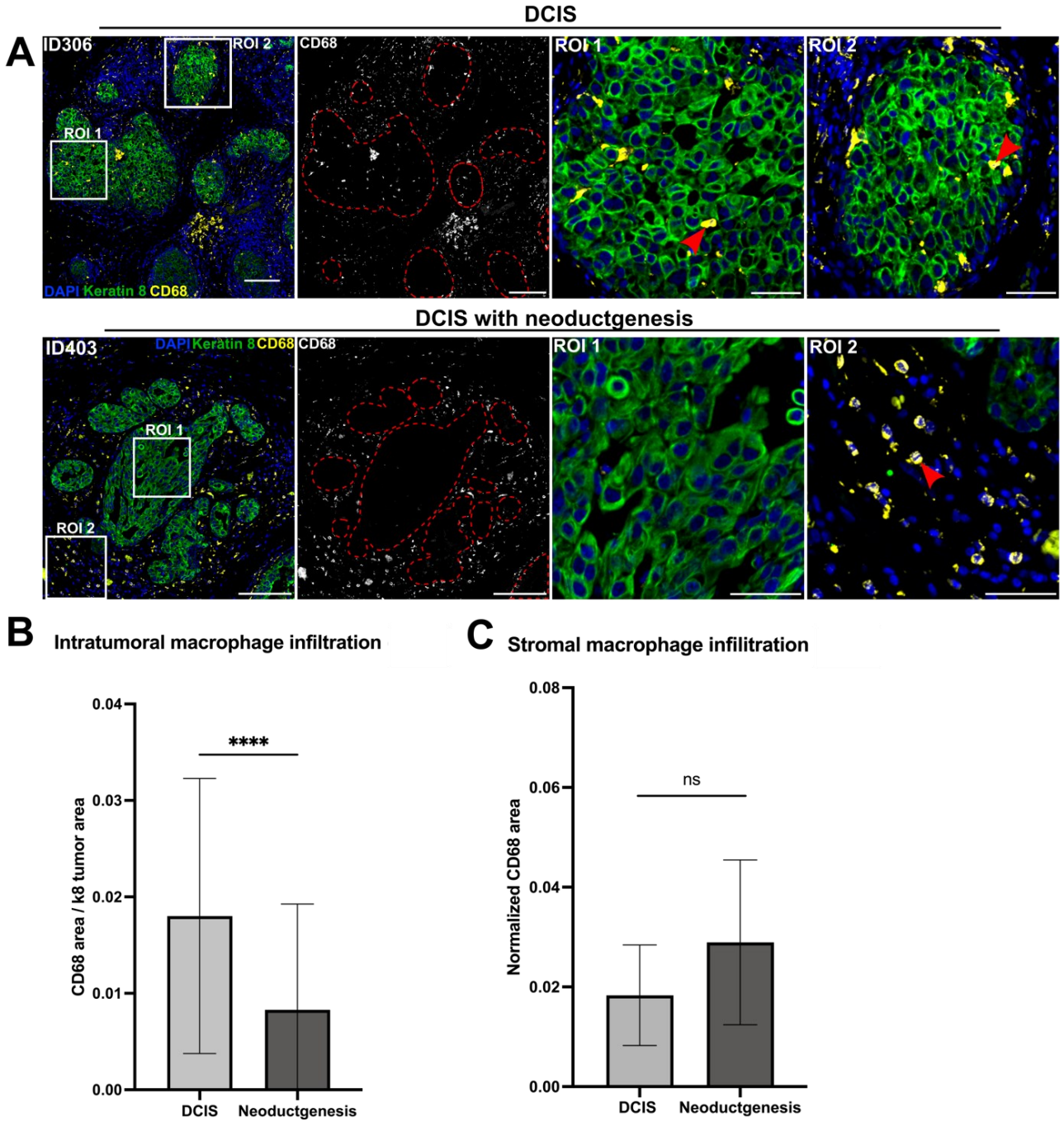

Figure 10. High grade DCIS tumors with neoductgenesis show significantly lower presence of intratumoral macrophages. Representative IF images of macrophage marker CD68 (yellow) (A), and quantification of the CD68 signal area normalized to total area of the tumor (B) and stroma (C) [mean ± SD, n(DCIS) = 10 FOVs from 4 patients, n(DCIS with neoductgenesis) = 11 FOVs from 3 patients]. Tumor and stroma were separated with the use of KRT8 (green; tumor border indicated with dashed lines). Nuclei were labelled with DAPI. Red arrowheads point to macrophages inside and outside of tumor (A). Neoductgenesis tumor samples exhibit significantly decreased presence of intratumoral macrophages ($p<0.0001$, Mann-Whitney U-test) (B) compared to conventional DCIS tumors. Neoductgenesis tumor samples exhibit higher levels of CD68-positive macrophages in tumor stroma compared to conventional DCIS tumors, but not statistically significantly ($p=0.1100$, Mann-Whitney U-test) (C). Scale bars: 150 μm and 50 μm in ROIs.

2.4 High grade DCIS tumors with neoductgenesis show abnormal expression pattern of the myoepithelial marker keratin 14 (KRT14)

In addition to αSMA labelling in IMC (Figure 6), IF staining of KRT14 was utilized for the evaluation of myoepithelial cell features of DCIS tumors with and without neoductgenesis. According to KRT14 staining, all examined DCIS tumors (n=2-3) showed myoepithelial cells surrounding the cancer cells at the edges of tumor acini separating cancer cells from the surrounding stroma (Figure 11). Interestingly, DCIS tumors with neoductgenesis exhibited abundant KRT14-positive cells among cancer cells, at the luminal side of the tumor, a feature not observed in conventional DCIS tumors (Figure 11). The distinct presence on KRT14-positive cells was seen inside the duct-like structures in both of the labelled neoductgenesis tumor samples.

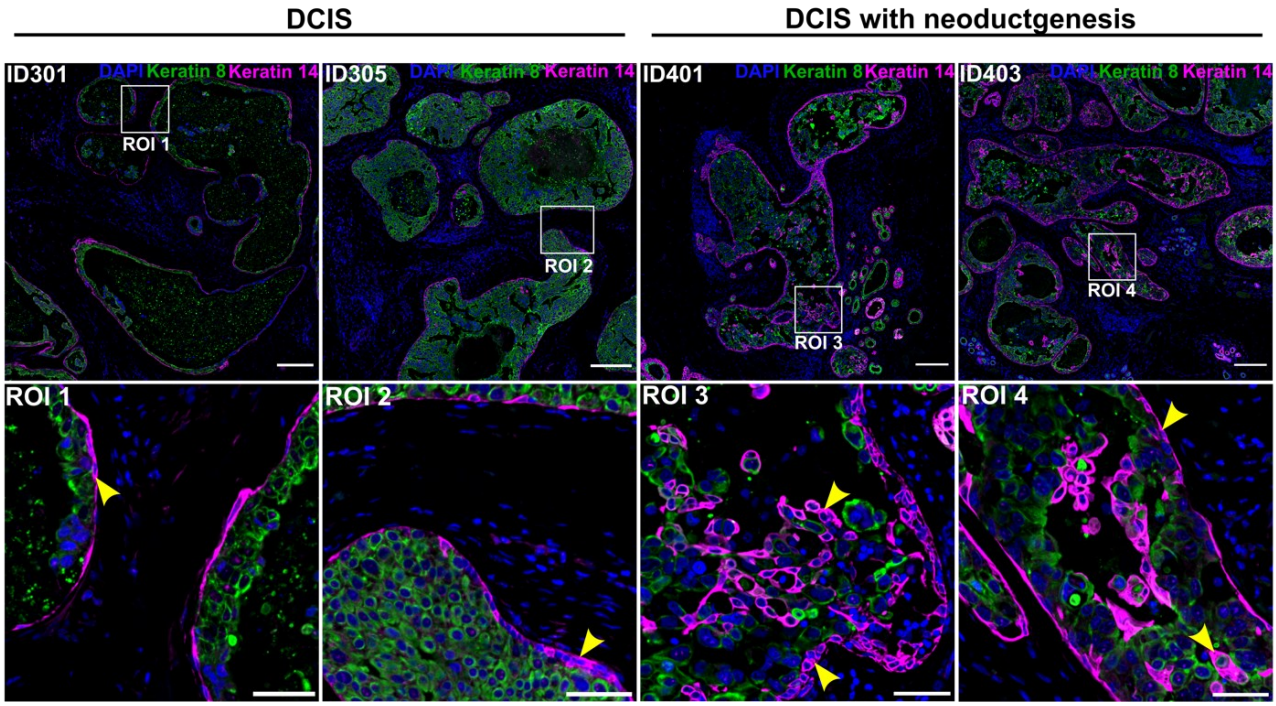

Figure 11. High grade DCIS tumors with neoductgenesis show abnormal myoepithelial cell features. Representative images of KRT14 IF staining. DCIS tumors with neoductgenesis [n(DCIS) = 9 FOVs from 3 patients, n(DCIS with neoductgenesis) = 7 FOVs from 2 patients] show abnormal location of KRT14-positive cells. Yellow arrowheads are pointing to KRT14-positive cells. In figures: KRT8 in green, KRT14 in magenta and DAPI in blue. Scale bars: 150 μm and 50 μm in ROIs.

2.5 Ds-sc-Fv-Fc antibody fragments inhibit the proliferation of breast cancer cell lines

Also patients with high grade DCIS, and particularly with neoductgenesis, could benefit from HER2-targeted therapies when the tumor has HER2 amplification. In this thesis, the efficacy of

disulfide bridge-stabilized scFv antibody fragments (ds-scFv-Fc) derived from trastuzumab were compared to the current trastuzumab used in the clinic. In the tested antibody fragments, trastuzumab scFv fragments have been fused to the Fc fragment and scFv part has been stabilized with a disulfide-bond. Two different ds-scFv-Fc fragments were examined; a bivalent ds-scFv-Fc antibody fragment with a stabilizing disulfide bond, and a tetravalent ds-scFv-Fc-ds-scFv fragment with four scFvs stabilized with disulfide bonds. In addition, two control fragments were utilized; an scFv-Fc fragment without an extra disulfide bond, and a VHR50A ds-scFv-Fc fragment predicted to have reduced binding affinity. The effectiveness of these therapeutic antibodies to inhibit cancer cell proliferation was analyzed to evaluate whether the ds-scFv-Fc antibody fragments have equal or even better efficacy compared to trastuzumab. The fragments could have improved pharmacological properties as a clinical settings due to their smaller size and hence better tissue penetration (Holliger and Hudson, 2005). In addition, the purpose was to investigate how the efficacy of these compounds differs in different breast cancer cells lines that are either HER2-positive or -negative, or trastuzumab-sensitive or -resistant. The quantification of cell proliferation under different treatments was measured during 4-5 days with IncuCyte imaging.

2.5.1 Trastuzumab impairs the proliferation of trastuzumab-sensitive BT474 cells

Four different breast cancer cell lines were utilized, BT474, MDA-MB-361 and JIMT-1 having HER2 amplification and MCF7 as a control cell line without HER2 amplification (Figure 12A). Within 96 hours, trastuzumab significantly ($p=0.0022$) inhibited the proliferation of HER2-positive and trastuzumab-sensitive BT474 cells compared to non-treated control (Figure 12B). Although, MDA-MB-361 and JIMT-1 are also HER2-positive, no similar effect were seen due to the resistance to trastuzumab (Tanner et al., 2005; Pietilä et al., 2019). As expected, trastuzumab had no significant effect on the proliferation capacity of MCF7 cells. (Figure 12B).

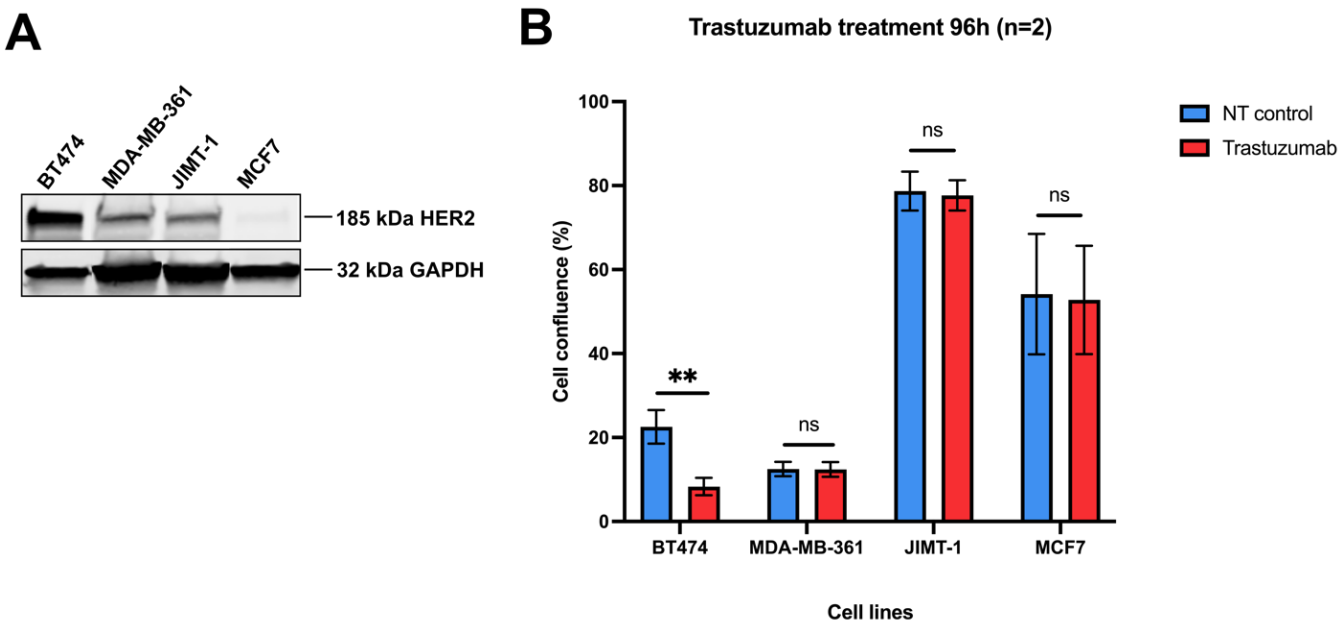

Figure 12. Trastuzumab impairs the proliferation of trastuzumab-sensitive BT474 breast cancer cells. Western blot analysis of HER2 expression in four different breast cancer cell lines: trastuzumab-sensitive BT474, and trastuzumab-resistant MDA-MB-361 and JIMT-1 cell lines with HER2 amplification, and MCF7 as a control cell line without HER2 amplification (A). GAPDH was used as loading control. Cells were treated with trastuzumab 50 μg/ml or left untreated (NT control) and cell proliferation was measured after 96-hours of trastuzumab treatment using IncuCyte imaging (B). Trastuzumab significantly inhibited the proliferation of BT474 cells (p=0.0022). (Mean ± SD, n=6, from two independent experiments, Mann Whitney U-test).

2.5.2 MDA-MB-361 cells are more sensitive to ds-scFv-Fc antibody fragments compared to the other trastuzumab-resistant breast cancer cell lines

The effectiveness of the novel ds-scFv-Fc therapeutic antibody fragments was quantified in different breast cancer cell lines to evaluate whether these antibody fragments with potentially improved pharmacological properties have equal or even better ability to inhibit the proliferation of HER2-positive breast cancer cells compared to trastuzumab. Each of four cell lines was cultured in vitro with different treatments for 5 days and proliferation of the cells was quantified using IncuCyte imaging software. Two individual experiments with three technical replicates per treatment were conducted. Statistical analyses were made using GraphPad Prism software and two-way ANOVA test was used for normally distributed data.

The in vitro data showed that trastuzumab significantly impaired the proliferation of trastuzumab-sensitive BT474 cells, as was expected (p=0.0001) (Figure 13A). In addition, scFv-Fc (p=0.0004), ds-scFv-Fc (p=0.0001) and ds-scFv-Fc-ds-scFv (p=0.0033) antibody fragments all significantly inhibited the proliferation of BT474 cells. Also the control fragment VHR50A dsscFv-Fc significantly inhibited the proliferation of BT474 cells (p=0.0006). As expected, trastuzumab had

no effect on the proliferation capacity of trastuzumab-resistant breast cancer cell line MDA-MB-361 (Figure 13B). Interestingly, scFv-Fc ($p<0.0001$), ds-scFv-Fc ($p=0.0003$) and ds-scFv-Fc-ds-scFv ($p<0.0001$) fragments all significantly inhibited the proliferation of MDA-MB-361 cells. Similar to BT474 cells (Figure 13A), the VHR50A ds-scFv-Fc significantly inhibited the proliferation of MDA-MB-361 cells ($p<0.0001$). In addition, the data show that neither trastuzumab nor any of the tested antibody fragments significantly affected the proliferation of HER2-positive but trastuzumab-resistant JIMT-1 cells (Figure 13C). The same response can be also seen in HER2-negative MCF7 cells where neither trastuzumab nor any of the fragments significantly affected the proliferation of MCF7 cells (Figure 13D). Interestingly, the proliferation capacity of MCF7 cells was significantly increased in the presence of tetravalent ds-scFv-Fc-ds-scFv fragment ($p=0.0297$).

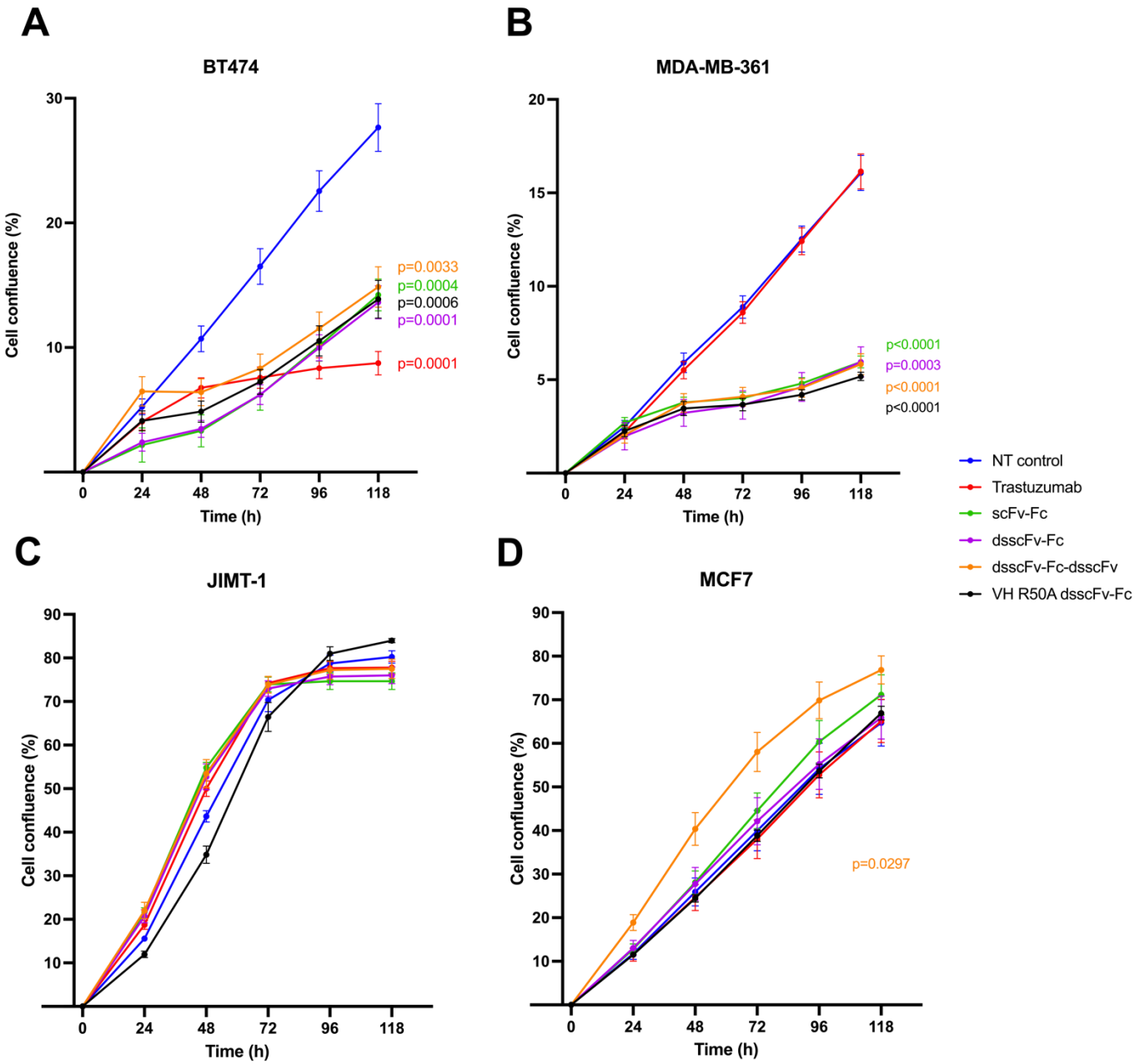

Figure 13. MDA-MB-361 cells are more sensitive to ds-scFv-Fc antibody fragments compared to other trastuzumab-resistant breast cancer cell lines. BT474 (A), MDA-MB-361 (B), JIMT-1 (C) and MCF7 (D) breast cancer cells were treated with trastuzumab (50 μg/ml) or the indicated ds-scFv-Fc antibody fragments (50 μg/ml) for 5 days. Cell confluence was monitored by Incucyte imaging. (Mean ± SEM, n=6 from two independent experiments, two-way ANOVA).

3 Discussion

3.1 High grade DCIS with suspected neoductgenesis exhibit abundant immune cell infiltration and HER2 receptor overexpression

Because of the current unmet clinical need to distinguish patients with neoductgenesis from other DCIS tumors, this thesis employed IMC and validation by IF to investigate the spatial molecular features of neoductgenesis. High grade DCIS tumor samples with and without neoductgenesis were obtained through collaboration with Turku University Hospital. The clinical evaluation of patient samples was conducted by a breast pathologist.

In this study, histopathological features specific to DCIS tumors with and without neoductgenesis were observed. According to pathologists, tumors with neoductgenesis fulfill the criteria of DCIS diagnosis because these tumors are observed as macroscopically and microscopically very similar. In this study, based on H&E staining tumors with and without neoductgenesis were also observed to be very similar. However, in neoductgenesis tumors closely packed, distorted tumor structures were observed. Increased collagen accumulation was observed around these duct-like tumor structures which is in accordance with previous studies (Tabár et al., 2022). In addition to the increased collagen accumulation, it has been shown that the orientation of collagen fibers changes during disease progression. Conklin et al. (2011) showed that the collagen fibers are adjacent to tumor margin in DCIS while in IDC collagen fibers are more perpendicularly orientated possibly helping cancer cells to invade to surrounding stroma (Conklin et al., 2011). However, in DCIS tumors with other poor prognostic markers, such as HER2-positivity perpendicularly localized collagen fiber are more present (Conklin et al., 2018). Hence, it would be interesting to investigate the organization of collagen fibers in the neoductgenesis tumors.

In general, high grade DCIS tumors are associated with an increased immune cell infiltration observed in tumor stroma (Thompson et al., 2016), which was also seen in the DCIS samples used in this study. In addition, the tumor samples with features of neoductgenesis showed thick lymphocytic infiltration surrounding these newly formed duct-like structures which is also in accordance with previous studies (Łazarczyk et al., 2023). Some of the tumors with features of neoductgenesis, for example ID406, had very strong immune cell infiltration in the stroma. This strong immune cell infiltration was observed particularly around the suspected neoducts not present in the conventional DCIS tumors. Breast cancers have for a long time been considered so-called “cold” tumors due to their low density of immune cells in the TME (Zhang et al., 2022). However,

for the past few years, new data has accumulated about the role of immune cells in the breast cancer microenvironment, and understanding the importance of immune cells in the treatment outcomes of breast cancer is starting to shift the consensus (Chen et al., 2024). However, it is less clear what the effect of the immune cells is in DCIS progression and what is their relevance to breast cancer prognosis due to the contradictory results (Pruneri et al., 2017). Toss et al. (2018) studied the prognostic significance of TILs based on their localization in DCIS tumors. They found that "touching TILs", in contact or very close to the basement membrane, were significantly associated with shorter recurrence-free interval compared to TILs that were further away from DCIS tumor acini (Toss et al., 2018). In addition, they showed that high density of TILs in the tumor stroma was associated with local recurrence and cancer progression in DCIS patients.

In this study, the immune cell infiltration was observed particularly around the duct-like structures very close to basement membrane of the tumor acini in neoductgenesis tumors. Hence, it would be interesting to further quantify the density of touching immune cells between the high grade DCIS tumors with and without neoductegenesis. The abundant stromal immune cell infiltration in tumor samples with neoductgenesis also indicates, that there could be opportunities to benefit from the current immune-oncological treatments that are intensifying the immune system to eliminate cancer cells. For example, TNBC is a breast cancer subtype that exhibits greater presence of immune cells in the TME compared to other breast cancer subtypes (Liu et al., 2018), and immune checkpoint inhibitor have been shown to be highly effective in the treatment of TNBC (Emens et al., 2020). Many immune checkpoint inhibitors have already been approved for the treatment of TNBC. These treatments may also have potential therapeutic effect in neoductgenesis tumors as well due to the immune cell rich TME. At the same time, the lack of macrophages inside the neoductgenesis tumor acini, observed in this study, could indicate mechanisms of immunosuppression.

The overexpression of HER2 receptor has previously been shown to be common in the neoducts (Tabár et al., 2022), and therefore the IHC staining of HER2 was performed. DCIS tumor samples with neoductgenesis used in this study showed overexpression of HER2 receptors which is in accordance with previous studies (Zhou et al., 2017; Tabár et al., 2022). The HER2 receptor status of two neoductgenesis tumor samples ID401 and ID403 was previously observed by a pathologist to be 3+ and our staining confirmed that. The HER2 staining of the third neoductgenesis sample ID405 was not successful due to the lack of tumor area in the tissue, but it seemed to be HER2-positive as well. The HER2 staining also showed that two of the DCIS tumor samples, ID301 and ID305, had also HER2 receptor overexpression. The DCIS tumor sample ID302 was the only sample with no HER2 overexpression. Since HER2 receptor overexpression is associated with a

more aggressive tumor phenotype (Thorat et al., 2021), abundant HER2 receptor overexpression in neoducts support its aggressive nature. As neoductgenesis tumors are currently under in situ diagnosis, the patients do not get the benefit from HER2 targeted therapies in the absence of proof for a significant therapeutic effect in HER2-positive DCIS (Cobleigh et al., 2021). Therefore in Finland, the HER2 targeted therapy is currently restricted to metastatic breast cancer. Due to the HER2 overexpression and the potentially aggressive and invasive nature of neoductgenesis, these patients could benefit from HER2-targeted therapies such as trastuzumab. In addition, as a breast conserving surgery may not represent an optimal treatment approach for these patients due to the large tumor burden of neoductgenesis, the significance of neoadjuvant/adjuvant therapies for such cases becomes paramount.

3.2 Increased vascularisation and loss of intratumoral macrophages may be associated with the aggressiveness of neoductgenesis

The formation of new blood vessels is significant for tumor growth and progression (Hanahan and Weinberg, 2011). According to results from IMC, increased vascularization was observed in the neoductgenesis tumors, and validation of CD31 immunolabelling in the whole tissue sections confirmed that. However, it is not known whether the significantly increased vascularization observed in the neoductgenesis tumors is newly formed blood vessels or whether the abundant vascularity is linked to a potentially different location of the tumor in the ductal part of the mammary gland, as previously proposed (Tabár et al., 2022). Previous studies have shown that the formation of new blood vessels in tumor stroma increases the risk of recurrence in DCIS patients (Teo et al., 2003). Therefore, it is likely that the higher vascularity of these tumors supports the invasive and aggressive nature of neoductgenesis.

In addition, the lack of intratumoral macrophages within the neoducts could support the aggressive nature of neoductgenesis. In this study, CD68+ macrophages were observed in the stroma and inside the tumor acini (intratumoral) of the conventional DCIS samples. However, the DCIS tumors with neoductgenesis showed significantly lower amount of intratumoral macrophages. Linde et al. (2018) investigated the role of intratumoral macrophages in intravasation of breast cancer cells. They showed that high grade DCIS tumors had significantly increased density of intratumoral macrophages compared to low-grade DCIS tumors (Linde et al., 2018). Linde et al. (2018) also showed that high density of intratumoral macrophages correlated with HER2 overexpression in mice. In this study, the HER2 overexpression and the number of intratumoral macrophages did not correlate. In fact, the only tumor sample ID302 without HER2 overexpression had the most

intratumoral macrophages. In general, the prognostic significance of the intratumoral macrophages in DCIS patients has not been investigated. However, Risom et al. (2022) showed that immune cells had better access to the tumors when the myoepithelial cell layer of DCIS tumors was thin and discontinuous, and this was associated with better outcome (Risom et al., 2022). In addition, Shinohara et al. (2022) showed that higher density of more M1-type CD68+ and PDL1-positive and CD163-negative intratumoral macrophages were associated with favourable clinical outcome in TNBC (Shinohara et al., 2022). Hence, it would be interesting to investigate the M1/M2 polarity of the intratumoral TAMs in DCIS and neoductgenesis tumors.

In this study, elevated density of stromal CD68+ macrophages was observed in the stroma of DCIS tumors with neoductgenesis, although this difference was not statistically significant. Although the significance of the stromal macrophages has been widely studied in breast cancer, less is known about the role of macrophages in DCIS. Increased density of stromal CD68+ macrophages was previously associated with invasive recurrence in patients with DCIS (Chen et al., 2020). Chen et al. (2020) also showed that especially higher density of CD163+ M2-type TAMs in tumor stroma was significantly associated with poorer disease-free survival in DCIS patients. Also, Jääskeläinen et al. (2024) showed that high number of CD163+ M2-type TAMs is independently associated with poor prognosis in patients with HER2-positive breast cancer (Jääskeläinen et al., 2024). Therefore, the number of M2 type TAMs in the stroma of neoductgenesis tumors would be a very interesting topic to investigate in the future. As higher presence of stromal macrophages has been linked to increased density of angiogenesis in the tumor stroma (Leek et al., 1996), the observed higher vascularity and the higher amount of macrophages in the stroma of neoductgenesis tumors could potentially be connected. However, this remains to be investigated.

3.3 Vimentin and Ki67 do not appear to be specific biomarkers for neoductgenesis

According to the IMC data, increased stromal vimentin was visually observed in the neoductgenesis tumors, but no significant difference was observed in quantitative image analysis. Vimentin is a type III intermediate filament protein mainly expressed by fibroblasts, immune cells and endothelial cells. It has been shown that vimentin has many functions in breast cancer. For instance, vimentin is involved in EMT which promotes the loss of cell-cell adhesion and increases cell migration (Mendez et al., 2010). It has also known that vimentin is enhances the invasion of breast cancer cells (McInroy and Määttä, 2007). In this study, vimentin expression was observed mostly in the stroma, and not in cancer cells. The strong density of stromal vimentin observed in neoductgenesis

tumors is likely linked to their increased immune cell infiltration but does not appear to be specific biomarker for neoductgenesis.

Increased cancer cell proliferation was also observed in the neoductgenesis tumors based on the IMC analysis. However, this finding could not be validated by IF imaging of Ki67 in whole tissue sections. In fact, some parts of neoductgenesis tumor areas had even lower cancer cell proliferation compared to conventional DCIS. It is possible that the areas that were selected for IMC had coincidentally more cancer cell proliferation. The maximum area selected for IMC analysis was allowed to be only 1 mm x 1 mm and while DCIS typically is very heterogeneous even within in single patient that small area does not represent the tissue in a whole. The density of Ki67 signal in fully scanned tissue slides appeared very similar between DCIS and neoductgenesis tumors supporting the fact that the areas selected for confocal microscopy imaging and quantification were representative. In all, large variation was observed in the proliferation of all analyzed tumors. Therefore, the proliferation of cancer cells does not appear to be a specific biomarker for neoductgenesis based on this study.

3.4 Atypical expression pattern of keratin 14 in neoductgenesis tumors might serve as a conceivable biomarker for neoductgenesis

In general, myoepithelial cell markers (αSMA, p63, KRT14) are important tools in breast cancer diagnostics to differentiate between invasive and localized (in situ) breast cancer. In early-stage breast cancer, the presence of a myoepithelial cell layer can be observed, while the loss of myoepithelial cell layer means that the cancer has invaded to surrounding stroma and hence is a hallmark of invasive breast cancer (Werling et al., 2003). Based on the IMC analysis, the expression of myoepithelial cell marker αSMA was evenly distributed around high grade DCIS tumors with and without neoductgenesis. Additionally, another myoepithelial cell marker KRT14 was utilized in the IF analysis of DCIS tumors. According to IF validation, KRT14-positive basal cell layer was observed surrounding DCIS tumors with and without neoductgenesis. Interestingly, high density of KRT14+ cells was consistently observed also inside the tumors with neoductgenesis. Based on their location, shape and KRT8 expression level, these cells appeared to be cancer cells. However, whether these cells are displaced normal basal cells or KRT14+ cancer cells with myoepithelial features remains to be further studied.

It has been shown that $KRT14^{high}$ basal cells are more prominent in ductal parts of mammary gland (Peurla et al., 2023). Additionally, KRT8+KRT14+ double-positive luminal epithelial progenitor

cells have been suggested to resign predominantly in the ductal parts of the human breast. As it has been suggested that neoductgenesis is originating from major lactiferous ducts rather than the TDLU structures where breast cancer often arises (Tabár et al., 2022), the presence of KRT14+ cells might be linked to this ductal origin. Collective invasion of breast cancer was previously also shown to be mediated by KRT14+ migratory cancer cells (Cheung et al., 2013; Cheung et al., 2016). Therefore, one hypothesis to be tested in the future experiments is whether the KRT14+ cells inside the neoducts are more migratory and thus form the new cancerous duct-like structures specific to neoductgenesis tumors.

There is growing evidence suggesting that myoepithelial cells around the DCIS tumors are immunophenotypically different compared to myoepithelial cells surrounding normal breast ducts and TDLUs. For instance, Hilson et al. (2009) showed that in some of the DCIS cases, the myoepithelial cells are expressing less SMA or cytokeratin 5/6, so the expression profile of the myoepithelial cell markers can be different between the DCIS tumors (Hilson et al., 2009). Hence, when studying the myoepithelial integrity of the neoductgenesis tumors it would be advisable to use more than one myoepithelial cell marker.

3.5 Ds-scFv-Fc antibody fragments show efficacy in HER2 targeting

Trastuzumab remains a cornerstone of the treatment of HER2-positive breast cancer. Despite its efficacy and the improvement of prognosis and quality of life in HER2-positive breast cancer patients, the development of drug resistance against trastuzumab remains a significant clinical problem (Ibragimova et al., 2024). Hence, there is an unmet need to provide solutions for improvement of the survival of patients with HER2-positive breast cancer. The potency of novel disulfide bridge-stabilized scFv-Fc antibody fragments derived from trastuzumab with potentially improved pharmacological properties and improved tumor penetration (Yokota et al., 1992) was explored in this thesis in comparison to trastuzumab.

Based on the results of this study, BT474 cell line was the only cell line sensitive to trastuzumab, as expected (Zazo et al., 2016). Although, MDA-MB-361 and JIMT-1 also have HER2 amplification, they are resistant to trastuzumab (Köninki et al., 2010). As trastuzumab does not cross the cell membrane, this resistance might be due to the different localization of HER2 receptors in cells. Indeed, it has been shown that MDA-MB-361 and JIMT-1 cells exhibit more intracellular HER2 compared to BT474, where the HER2 receptors are more localized to the plasma membrane (Pietilä et al., 2019).

All of the ds-scFv-Fc antibody fragments tested in this study significantly inhibited the proliferation of trastuzumab-sensitive BT474 cells, although they had inferior potency to suppress the proliferation compared to trastuzumab. Although the tetravalent fragment has two times more binding sites compared to bivalent antibody fragment, its ability to inhibit the proliferation of BT474 cells was weaker compared to bivalent antibody fragment. Interestingly, the scFv-Fc control fragment without the stabilizing disulfide bond and the VHRO50A as control fragment with reduced binding affinity also induced significant reduction in BT474 cell proliferation. Based on this, it is possible that the stabilizing disulfide bond in the sc-part of antibody may not be necessary. Furthermore, it appears that the binding affinity of VHRO50A control fragment may not be very much lower compared to the other tested antibody fragments, which should be further evaluated. In future studies, it would be important to include control fragments that are not targeted to HER2.

As expected, neither trastuzumab nor the ds-scFc-Fc antibody fragments inhibited the proliferation of MCF7 cells. Interestingly, the tetravalent (ds-scFv-Fc-ds-scFv) fragment significantly increased the proliferation capacity of MCF7 cells compared to non-treated control. This effect was not seen in the other cell lines. The concentration of the tetravalent fragment was also two to three times lower compared to other fragments, so the volume added to the cells was two-fold. Hence, one possibility is that the increased volume (PBS) of the cultures increased the proliferation of these cells somehow.

This study also demonstrates that all the tested ds-scFv-Fc fragments significantly inhibited the proliferation of trastuzumab-resistant MDA-MB-361 cells, while neither of the antibody fragments affected the proliferation of JIMT-1 cells. The reason why trastuzumab-resistant cell lines MDA-MB-361 and JIMT-1 are responding differently to ds-scFv-Fc fragments might be due their different cell line-specific properties. One of the factors influencing this may be the expression of sorting-related receptor (SORLA) in the breast cancer cells. SORLA is intracellular sorting protein which regulates the localization of HER2 receptors. Pietilä et al. (2019) have investigated the role and expression of SORLA in carcinoma cells and they showed that cells with high levels of SORLA have more HER2 receptor localized at the plasma membrane. They investigated the levels of SORLA in different breast cancer cell lines and found that trastuzumab-sensitive BT474 cells had highest SORLA levels on cell surface, MDA-MB-361 had intermediate whereas JIMT-1 cells had lowest expression of SORLA. (Pietilä et al., 2019). The fact that MDA-MB-361 have higher expression of SORLA than JIMT-1 cells and hence more plasma membrane-localized HER2 receptors (Pietilä et al., 2019) could potentially explain the difference between the response to the ds-scFv-Fc fragments.

Köninki et al. (2010) also showed that both JIMT-1 and MDA-MB-361 cell lines have a mutated PIK3CA gene and low phosphatase and tensin homolog (PTEN) mRNA levels (Köninki et al., 2010). Although trastuzumab binds to HER2 receptors, mutated PIK3CA gene is keeps the PI3K-Atk signalling cascade active which is enhancing cancer cell survival (Junttila et al., 2009). Köninki et al. (2010) also showed that JIMT-1 cells have high expression of neuregulin 1 (NRG1) which has been shown to be one of the resistance mechanisms to trastuzumab (Yang et al., 2017). This might be the reason why JIMT-1 cells with high expression of NRG1 are able to avoid the effect of these antibody fragments.

The fact that ds-scFv-Fc fragments had superior potency to suppress the proliferation of MDA-MB-361 cells compared to trastuzumab means that the fragments must somehow affect the cells differently from trastuzumab. Possible explanations include the smaller size of the fragments with improved binding kinetics. However, the tetravalent fragment has approximately the same size as trastuzumab (approx. 150 kDa) and still was superior in efficacy compared to trastuzumab. This finding could be also related to the binding affinity of the fragments. With higher affinity the fragments could bind to HER2 better than trastuzumab or even bind in different part of the HER2 receptor, which would allow them to block for example HER2-HER3 heterodimerizations, that has been shown to promote breast cancer proliferation (Lee-Hoeflich et al., 2008). The binding affinity of the fragments compared to trastuzumab remains to be evaluated.

Taken all together, while more investigation needs to be done, these novel ds-scFv-Fc antibody fragments may offer clinical opportunities against trastuzumab-resistance as future therapeutic antibodies. Since, breast cancer is in general very heterogeneous, those patients that do not respond to trastuzumab or other HER2-targeted therapies could possibly benefit from these antibody fragments.

3.6 Limitations of this study

One significant limitation of this study is the small size of the discovery set of tumor samples. To really evaluate the significance of the observed neoductgenesis-specific molecular features, these results need to be validated in a bigger sample cohort of high grade DCIS tumors. In addition, a limitation associated with small sample size is that the variability within the samples might obscure some of the differences besides decrease the statistical power of this study.

The number of images taken for quantitative image analysis could also affect the statistical power of this study, as the samples are very heterogenous. More comprehensive analysis of the tissue

sections would thus be beneficial. In addition, IF staining of tissues involves autofluorescence which can interfere with the detection of specific signal. Especially, when tumor and stromal areas were separated with the KRT8 signal, some unspecific signal was observed in the stroma which disturbed the quantifications. Human bias may also have affected image quantification as the imaged areas were selected and segmented manually.

4 Conclusion

In this master's thesis the specific histopathological and molecular features of neoductgenesis were investigated. The analysis of patient samples revealed molecular features that are in line with the reports of aggressive and invasive nature of neoductgenesis, namely HER2 overexpression, significantly increased stromal vascularity, and significant loss of intratumoral macrophages. Another very important finding was that neoductgenesis tumors showed abundant KRT14-positive cells inside the duct-like tumor structures, which could indicate its distinct origin. The findings of this study may serve as potential biomarkers for neoductgenesis in the future.

In addition, in this master's thesis, the efficacy of disulfide bridge-stabilized scFv antibody fragments was compared to trastuzumab used in the clinic. The aim was to assess their capacity to inhibit the proliferation of HER2-positive breast cancer cells to ultimately offer alternative solutions to overcome trastuzumab resistance. These novel ds-scFv-Fc antibody fragments showed superior efficacy to inhibit the proliferation of trastuzumab-resistant but HER2-positive breast cancer cells. Hence, these fragments may have clinical potential to battle against trastuzumab resistance as future therapeutic antibodies in both HER2-positive breast cancers as well as other cancers with HER2 amplification.

The results obtained from this study indicate that neoductgenesis has specific molecular features that may explain its distinct and invasive nature and hence it would be very important that patients with neoductgenesis could receive the correct diagnosis and the best possible treatment according to their needs. Further research is needed to validate the existing biomarkers and discover new ones as well as investigate the molecular mechanism behind this phenomenon. However, these findings hold potential to differentiate the patients with neoductgenesis from DCIS in the future as well as advance our comprehension of the underlying molecular mechanisms behind this phenomenon.

5 Materials and Methods

5.1 Tumor samples

Clinical tissue material was obtained from patients undergoing breast cancer surgery through our established collaboration with Turku University Hospital. Tumor samples have been clinically evaluated by radiologists and pathologists (Table 1). All breast tissue donors provide written informed consent for the tissue collection. The protocol has been ethically approved by Varha (Dnro: 23 /1801/2018 with amendments 20.3.2018, 19.2.2019, and 17.1.2023) and permitted by the Turku University Hospital (T107/2018-1).

Table 1. Detailed description of DCIS tumor samples with and without neoductgenesis used in this study.

According to diagnoses made by pathologist, ID30X samples represent conventional DCIS tumor samples and ID40X samples represent DCIS tumor samples with suspected neoductgenesis. The HER2 receptor status was clinically determined from four tumor samples. Six of the tumor samples were used for the IMC analysis and seven of the tumor samples were used for the IF staining.

Patient ID	Diagnosis	HER2 status	IMC	IF
ID301	Extensive DCIS GII-III + IDC focus GII	+++	x	x
ID302	DCIS GII-GIII	n/a	x	x
ID305	DCIS GIII	n/a	x	x
ID306	DCIS GII-III	n/a		x
ID401	Atypical DCIS GIII + suspected invasion	+++	x	x
ID403	DCIS GIII and IDC GIII	+++	x	x
ID405	DCIS GIII	n/a	x	
ID406	DCIS GII	+++		x

5.2 Molecular profiling of tumor samples with IMC

FFPE tissue samples from six different patients were selected for the IMC analysis (Figure 14A). Representative part of each tumor was selected based on the H&E figures, and FFPE blocks of tumor tissues were sectioned into 5 µm and transferred to glass slides. Three of the FFPE tissue samples represented high grade DCIS (ID30X) and three FFPE tissue samples represented high grade DCIS with features of neoductgenesis (ID40X) according to pathologists' evaluation (Figure 14B). FFPE tissue sections were stained using a pre-designed panel containing 28 metal-conjugated

antibodies (Fluidigm) against human structural feature proteins and immune cell markers (Figure 14C). Tissue sections were stained using general IF protocol. Briefly, deparaffinization was done with xylene and tissue sections were rehydrated with a series of decreasing ethanol dilutions. Antigen retrieval was conducted by incubating the tissue sections in pressure cooker for two hours in citrate buffer (Target Retrieval Solution, Citrate pH 6, Agilent Dako). The sections were then washed with Milli-Q water and blocked for 45 min in blocking buffer (10% FBS-PBS). Metal conjugated antibodies were diluted in blocking buffer as optimized to human breast cancer tissue and some dilutions used were based on the manufacturers' recommendation (Figure 14C). Slides were then incubated o/n in a humidified chamber at +4°C. On the next day, sections were washed twice with 0.2% Triton X-100 in PBS followed by washes with PBS. Then sections were incubated with Cell-ID (Intercalator-103Rh, dilution 1:200) in PBS for 30 minutes at room temperature (RT) and then washed with Milli-Q water and dried and stored at RT before analysis. For IMC analysis, areas (max. 1 mm x 1 mm) were selected according to the H&E slides of the tumor samples, concentrating on for instance interesting looking tumor structures with strong immune cell infiltration. Two ROIs per each section were selected and these areas were analyzed with the Hyperion IMC system (Fluidigm) at Imaging mass cytometry Core Facility in Turku, Finland. Briefly, the selected areas were ablated with a laser and the ablated materials were transferred to the mass cytometer which then measured the metal isotopes with time-of-flight technology at 1μm^2 resolution. The data was exported as MCD files and visualized using MCD viewer software (1.0.560.6, Fluidigm).

A

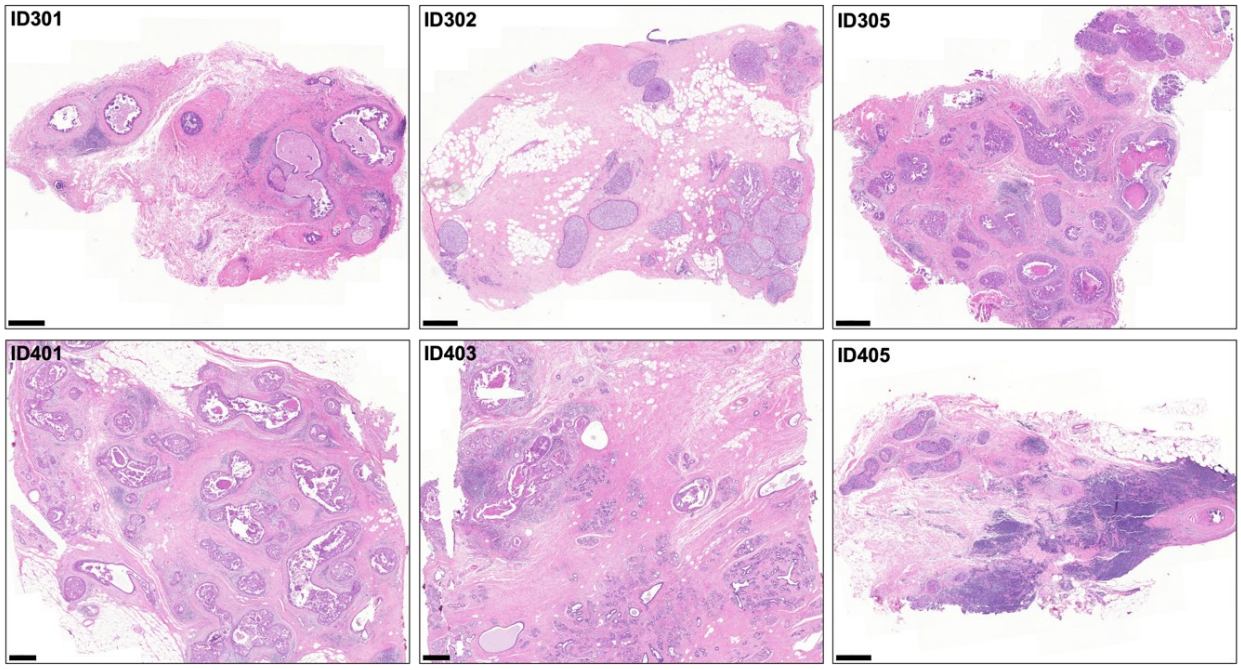

B

Patient ID	Diagnosis
ID301	Extensive DCIS GII-III + IDC focus GII
ID302	DCIS GII-GIII
ID305	DCIS GIII
ID401	Atypical DCIS GIII + suspected invasion
ID403	DCIS GIII + IDC GIII
ID405	DCIS GIII

C

Tag/Conj.	Antigen	Clone	Target species	Dilution
141Pr	α-Smooth Muscle Actin	1A4	anti-human	1:400
142Nd	CD19	6OMP31	anti-human/mouse	1:100
143Nd	Anti-Vimentin	D21H3	anti-human/mouse	1:400
144Nd	CD14	EPR3653	anti-human	1:100
146Nd	CD16	EPR16784	anti-human	1:50
148Nd	Pan-Kreatin	C11	anti-human	1:50
149Sm	CD11b	EPR1344	anti-human/mouse	1:50
150Nd	CD274/PD-L1	SP142	anti-human	1:50
151Eu	CD31/PECAM-1	EPR3094	anti-human	1:100
152Sm	CD45	D9M8I	anti-human	1:100
153Eu	CD223/LAG-3	D2G40	anti-human	1:50
[illegible]	CD11c	0,13125	anti-human	
155Gd	FoxP3	PCH101	anti-human	1:100
156Gd	CD4	EPR6855	anti-human	1:100
158Gd	Anti-E-Cadherin	24E10	anti-human/mouse	1:100
159Tb	CD68	KP1	anti-human	1:100
161Dy	CD20	H1	anti-human	1:200
165Ho	CD279/PD-1	EPR4877(2	anti-human	1:50
167Er	Granzyme B	EPR20129-	anti-human	1:100
168Er	Anti-Ki-67	B56	anti-human/mouse	1:100
169Tm	Anti-Collagen Type I	Polyclonal	anti-human/mouse	1:400
170Er	CD3	Polyclonal,	anti-human	1:100
171Yb	CD27	EPR8569	anti-human	1:100
[illegible]	Anti-Histone 3	D1H2	anti-human/mouse	
173Yb	CD45RO	UCHL1	anti-human	1:50
163Dy	Prox1	EPR19273	anti-human	1:50
164Dy	Lyve-1	EPR21857	anti-human	1:50
162Dy	Podoplanin	D2-40	anti-human	1:50
	Cell ID			1:200

Figure 14. Six different FFPE patient samples were selected for the IMC analysis. Patient sample panel consists of three high grade DCIS (ID30X) tumors and three high grade DCIS tumors with features of neoductgenesis (ID40X) (A). Patient samples have been evaluated by pathologist (B). FFPE tissue sections were stained using pre-designed antibody panel containing 28 metal-labelled antibodies against human structural feature proteins and immune cell markers (C). Part of the dilutions were optimized to human breast cancer tissue and some dilutions used were based on the manufacturers' recommendation as starting concentration.Scale bars: 500 μm.

5.3 Validation of markers detected with IMC using IF

According to the IMC results visually evaluated with MCD viewer software, five different markers were chosen based on their different appearance in both ROI areas between DCIS and DCIS with

neoductgenesis samples. FFPE tissue sections from seven different patients were utilized for the validation set, four DCIS tumor samples (ID30X) and three neoductgenesis tumor samples (ID40X) (Figure 15A, B). Three antibody panels were designed including antibodies for the five selected markers and common structural markers of mammary tissue (Figure 15C). For IF staining of these markers, first FFPE blocks were cut into 5 µm thick tissue sections, then deparafinized with xylene and rehydrated with decreasing ethanol gradient. Antigen retrieval was conducted by boiling slides in citrate buffer for 2 hours in pressure cooker. Then tissue sections were moved to PBS and before blocking microscope glass was carefully dried with soft tissue and PAP-pen was used to draw circle around the tissue sections. Then tissue sections were blocked 1h using 10% FBS-PBS. In first antibody panel, seven tissue sections were stained by primary antibodies against KRT8 (Troma-I, TROMA-I-c, Hybridoma Bank, dilution 1:800), CD31 (EPR3094, ab76533, Abcam, dilution 1:100) and CD68 (KP1, ab955, Abcam, dilution 1:200). In second antibody panel, seven tissue sections were stained by primary antibodies against KRT8 (Troma-I, TROMA-I-c, Hybridoma Bank, dilution 1:800), Ki-67 (GR3375556-1, ab15580, Abcam, dilution 1:250) and vimentin (V9, 347M-1, Sigma, dilution 1:1000). In third antibody panel, 5 tissue sections (ID301, ID302, ID305, ID401 and ID403) were stained by primary antibodies against KRT8 (Troma-I, TROMA-I-c, Hybridoma Bank, dilution 1:800), KRT14 (905301, Biolegend, dilution 1:1000) and CD45 (MEM-28, ab8216, Abcam, dilution 1:200). Primary antibodies were incubated 1 hour in RT and then overnight at 4°C in 10% FBS-PBS. Then tissue sections were washed 3 x 5 min with PBS and secondary antibodies against rat (Alexa Fluor 488 (A21208), Invitrogen), rabbit (Alexa Fluor 568 (A10042), Invitrogen) and mouse (Alexa Fluor 647 (A31571), Invitrogen) were diluted 1:400 in 10% FBS-PBS and incubated 1 hour in RT in humidified chamber protected from light. Secondary controls were included. Then tissue sections were washed with PBS 1 x 5 min and incubated with DAPI (Invitrogen, 1:1000) in PBS 10 min in RT e. Then tissue sections were washed with PBS 2 x 5 min and rinsed with dH20 before mounting. Tissue sections were mounted with Mowiol® (Calbiochem) supplemented with 2.5% 1,4-diazabicyclo(2.2.2)octane (DABCO, Sigma-Aldrich) and stored at RT protected from light. The labelled tissue sections were first scanned with Pannoramic Midi fluorescence slide scanner and then randomly selected interesting looking areas of the tissue sections were imaged with 3i Marianas CSU-W1 spinning disk confocal microscope (Intelligent Imaging Innovations, Inc.), equipped with a Photometrics Prime BSI sCMOS camera (2048x2048 pixels), and image acquisition was performed with Slidebook 6 software, where 2-4 FOVs were imaged per tissue sample using identical microscope settings and identical exposure times within different panels. The images acquired with Zeiss Plan-Apochromat 20x/0.8 NA objective. DAPI was excited with 405nm solid state laser, and emission captured with a 445/45nm filter. KRT8 was

excited with 488 nm solid state laser, and emission captured with a 525/30nm filter. CD31, Ki67 and KRT14 were excited with 568nm solid state laser, and emission captured with 617/73nm filter. CD68, VIM and CD45 were excited with 647nm solid state laser, and emission captured with 692/40nm filter.

A

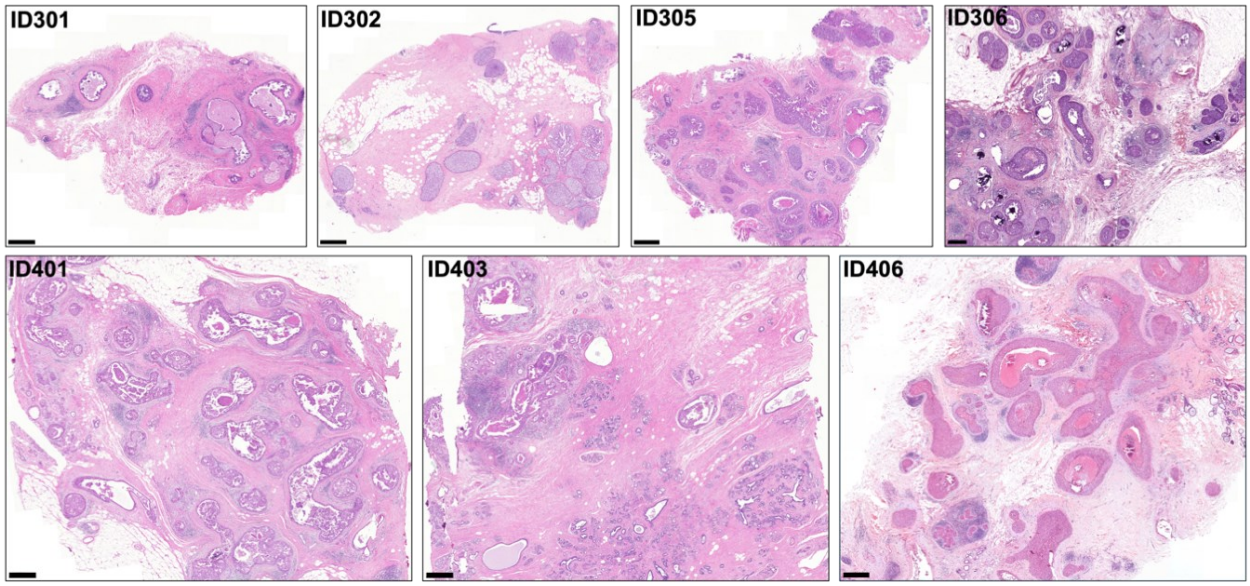

B

Patient ID	Diagnosis
ID301	Extensive DCIS GII-III + IDC focus GII
ID302	DCIS GII-GIII
ID305	DCIS GIII
ID306	DCIS GII-III
ID401	Atypical DCIS GIII + suspected invasion
ID403	DCIS GIII + IDC GIII
ID406	DCIS GII

C

Panel 1	Panel 2	Panel 3
Keratin 8	Keratin 8	Keratin 8
CD31	Ki67	Keratin 14
CD68	Vimentin	CD45

Figure 15. FFPE tissue sections from seven different patients were utilized for the IF validation set. Patient sample set consist of four DCIS tumor samples (ID30X) and three neoductgenesis tumor samples (ID40X) (A). Patient samples have been evaluated by pathologist (B). Three antibody panels were designed including antibodies for the five selected markers and common structural markers of mammary tissue (C). Scale bars: 500 μm.

5.4 Image quantification and statistical analysis

To determine the difference in the amount of proliferation between DCIS tumors and DCIS tumors with neoductgenesis, the area of intratumoral Ki67 was quantified from both sample groups. Tumor areas in the images were first segmented according to KRT8 signal labelling the epithelium, and nuclei signal inside the tumor areas were segmented according to DAPI signal. Ki67 signal was then tresholded and measured within the tumor, and normalized to the relative area of nuclei. Data

normality was assessed with Shapiro-Wilk normality test, and Mann-Whitney U-test was performed to assess the statistical significance of the results.

Similarly, to determine the difference in the amount of CD68+ intratumoral macrophages, tumor area was segmented according to KRT8 signal as above. Intratumoral CD68 signal was then thresholded, measured and then normalized to the relative tumor area. Data normality was assessed with Shapiro-Wilk normality test, and Mann-Whitney U-test was performed to assess the statistical significance of the results.

Finally stromal CD68+ macrophages, vimentin and CD31 signal were quantified by segmenting the tumor area according to KRT8 signal, inverting the results to obtain stromal area. The stromal CD68+ macrophages, VIM and CD31 signals were then tresholded, measured and normalized to the relative area of stroma. Data normality was assessed with Shapiro-Wilk normality test, and un unpaired T-test was performed to assess the statistical significance of the results. Image analysis was performed using ImageJ software (version 2.1.0/1.53c), and statistical analyses were conducted with GraphPad Prism (version 10.0.0).

5.5 IHC staining of HER2

HER2 IHC staining was utilized to determine the HER2 status in DCIS tumors with and without neoductgenesis. The routine staining of HER2 was conducted in the service of Histocore for six tumor samples, the same used for IMC. First, FFPE tissue sections were deparaffinized and rehydrated followed by antigen retrieval in pressure cooker (Decloaking chamber, Biocare Medical NxGen) with citrate buffer (pH 6, BioSite BSC-OKHURL) in 20 minutes. Blocking was conducted at RT using endogenous enzyme block (hydrogen peroxide) and pre protein block (WellMed BD09-125). The HER2 staining (HER2 A0485, Dako, dilution 1:250) was conducted in (semi)automate Labvision autostainer (Thermo-Fisher Scientific) with 1 h incubation at RT.

5.6 Analysis of cell proliferation and viability in vitro

5.6.1 Cell lines and culture conditions

Four different cells breast cancer cell lines were selected for the experiment. HER2-positive cell lines BT474, MDA-MB-361 and JIMT-1 as well as HER2 negative cell line MCF7 were maintained in DMEM/F12 Glutamax^{TM} (Gibco) supplemented with 10% fetal bovine serum (FBS) and 1% penicillin-streptomycin and cultured in 10cm cell culture flasks at 37°C with 5% CO2 and

95% humidity. Cells were passaged weekly using 0.25% trypsin-EDTA (Gibco). Cells were checked for the absence of mycoplasma contamination.

5.6.2 Western blot

To determine the HER2 expression profile of these cell lines, cell pellets were collected from each of the cell lines and lysates were made. Protein concentrations were measured using BioRad kit and the absorbance were measured with Ensight plate reader, and the protein concentrations of cell lysates were balanced. The samples were prepared for the western blot run by adding 6x SDS sample buffer to the lysates and boiling them at 95 °C for 10 min. Then samples were loaded on a 10-well 4-20% Mini-PROTEAN TGX gel (BioRad) and run 15 min at 100 V and then 45 min at 130 V to separate the proteins by size. After the run, proteins were transferred to TransBlot Turbo Mini PVDF membrane (Bio-Rad) by using TransBlot Turbo transfer system (BioRad) and program for large proteins. After transferring, membrane was blocked in 5% BSA in 0.1% TBS-Tween for 1 h at RT to avoid nonspecific binding. The primary antibody against HER2 (1:1000) was diluted in blocking buffer (1:1000) and the membrane was incubated in the primary antibody solution overnight at 4°C. The membrane was also incubated with primary antibody against GAPDH (5G4cc, HyTest, 1:2000) for 1 h at RT. The membrane was incubated in anti-rabbit secondary antibody (926-68073, IRDye, 1:4000) and anti-mouse secondary antibody (926-32212, IRDye, 1:4000) diluted in blocking buffer for 1 h at RT. Washes were conducted after primary and secondary antibody incubations with 5% BSA in 0.1% TBS-Tween for 3 x 5 min. The protein detection was conducted with Odyssey CLx imaging system (LI-COR).

5.6.3 Optimization of cell plating density and dose selection of trastuzumab

The sufficient plating density was evaluated for the main experiment. For the evaluation 5000, 10 000, 15 000, 20 000 and 25 000 cells per well of BT474, MDA-MB-361 and JIMT-1 cell lines were plated on a 96 well plate. In addition, 10 000, 15 000, 20 000 and 25 000 cells per well of MCF7s were plated on a 96 well plate. Plates were then incubated 72 hours at 37°C with 5% CO2 and 95% humidity and the proliferation of cells were detected with IncuCyte imaging system (10.65.14.2, IncuCyte S3, Sartorius). Optimal dose for trastuzumab were also evaluated. For optimal dose selection, trastuzumab-sensitive BT474 cells were plated on a 96 well plate, 10 000 cells per well with three replicate wells. On the following day the cells were treated with Trastuzumab (Trastuzumab A2007 in PBS pH 7.2, Sellechem) concentrations of 1, 5, 10, 50 ug/ml. The proliferation of the cells was monitored with IncuCyte imaging system as above.

5.6.4 Analysis of cell proliferation in the presence of trastuzumab and ds-scFv-Fc antibody fragments

BT474, MDA-MB-361, JIMT-1 and MCF7 were plated on 96-well plate at a density of 10 000 cells/well with three replicates and incubated overnight to achieve adherent cell layer. On the following day, the cells were treated with trastuzumab and two ds-scFv-Fc antibody fragments (in PBS, pH 7.4) and two control fragments derived from trastuzumab (Trastuzumab A2007 in PBS pH 7.2, Sellechem) in concentration of 50 ug/ml diluted in culture medium (200 ul per well); 1) Trastuzumab (A2007, Sellechem), 2) bivalent ds-scFv-Fc antibody fragment derived from trastuzumab, 3) tetravalent ds-scFv-Fc antibody fragment derived from trastuzumab, 4) scFv-Fc antibody fragment without extra disulfide bond and 5) inactivated VH R50A ds-scFv-Fc fragment, all produced at the lab of Urpo Lamminmäki. Plates were incubated for 5 days (120 h) at 37°C with 5% CO2 and 95% humidity and cell proliferation was monitored with IncuCyte imaging system. Two independent experiments were conducted.

5.6.5 Quantification of cell proliferation and statistical analysis

The quantification of cell proliferation was made using IncuCyte imaging software. New analysis definition was made to determine the confluence in six different time points for each of the cell lines separately. Confluence at each timepoint and condition was determined using representative images of each cell line and visually defining the analysis settings so that the cell confluence was measured appropriately from the representative images. The defined settings were then applied to the whole experimental data. The data was visualized, and statistical analysis performed using GraphPad Prism (version 10.0.0) software. Two-way ANOVA was used to determine the statistical differences between the treatments to inhibit the proliferation of these breast cancer cells lines.

Acknowledgements

I sincerely want to thank my supervisors, Emilia Peuhu and Laura Lehtinen, for the excellent guidance and support throughout this project. Especial thanks to Emilia Peuhu for making this project possible and Laura Lehtinen for providing me excellent guidance in the lab, as well as patiently answering my endless questions. Overall, I am very grateful for being part of this wonderful project and for having the opportunity to learn so many new things regarding breast cancer, especially the existing unmet needs regarding its treatment and clinical diagnostics. I am very grateful that I was able to explore specific diagnostic biomarkers for neoductgenesis, which may have great potential to improve the current DCIS diagnostics in the future.

I am also very grateful to the entire Peuhulab team: Defne Dinc, Emmi Hirvonen, Leena Koskinen, Markus Peurla and Oona Paavolainen. Thank you for being helping me whenever I needed it. Also, thank you for the awesome retreats that we did together, I really enjoyed them. I have truly felt that I am an important part of this team.

Thanks to my friends for all the support I have received during this process, especially my dear friends who has been in the same situation and provided valuable peer support for each other. Especially, thanks to my lovely family for supporting me through this process. Because my family never stopped believing in me throughout this process, neither did I.

Abbreviations

αSMA	Alpha-smooth muscle actin
DCIS	Ductal carcinoma in situ
ds-scFv-Fc	Disulfide bridge-stabilized single-chain variable fragment
ECM	Extracellular matrix
EMT	Epithelial-mesenchymal transition
ER	Estrogen receptor
FFPE	Formalin-fixed paraffin-embedded
HER2	Human epidermal growth factor receptor 2
IDC	Invasive ductal carcinoma
IF	Immunofluorescence
IHC	Immunohistochemistry
IMC	Imaging mass cytometry
KRT8	Keratin 8
KRT14	Keratin 14
ROI	Region of interest
scFv	Single-chain variable fragment
SORLA	Sorting-related receptor
TAM	Tumor-associated macrophages
TDLU	Terminal ductal lobular unit
TIL	Tumor infiltrating lymphocyte
TME	Tumor microenvironment
TNBC	Triple-negative breast cancer

TN-C	Tenascin C
PIK3CA	Phosphatidylinositol-4,5-bisphosphate 3-kinase catalytic subunit alpha
PI3K-Akt	phosphoinositide 3-kinase
PR	Progesterone receptor
VIM	Vimentin

References

Adams, M., J.L. Jones, R.A. Walker, J.H. Pringle, and S.C. Bell. 2002. Changes in tenascin-C isoform expression in invasive and preinvasive breast disease. *Cancer Res.* 62:3289–3297.

Albanell, J., and J. Baselga. 1999. Trastuzumab, a humanized anti-HER2 monoclonal antibody, for the treatment of breast cancer. *Drugs Today Barc. Spain 1998*. 35:931–946.

Alkabban, F.M., and T. Ferguson. 2024. Breast Cancer. *In* StatPearls. StatPearls Publishing, Treasure Island (FL).

Allinen, M., R. Beroukhim, L. Cai, C. Brennan, J. Lahti-Domenici, H. Huang, D. Porter, M. Hu, L. Chin, A. Richardson, S. Schnitt, W.R. Sellers, and K. Polyak. 2004. Molecular characterization of the tumor microenvironment in breast cancer. *Cancer Cell*. 6:17–32. doi:10.1016/j.ccr.2004.06.010.

Ayoub, N.M., S.K. Jaradat, K.M. Al-Shami, and A.E. Alkhalifa. 2022. Targeting Angiogenesis in Breast Cancer: Current Evidence and Future Perspectives of Novel Anti-Angiogenic Approaches. *Front. Pharmacol.* 13:838133. doi:10.3389/fphar.2022.838133.

Biswas, S.K., S. Banerjee, G.W. Baker, C.-Y. Kuo, and I. Chowdhury. 2022. The Mammary Gland: Basic Structure and Molecular Signaling during Development. *Int. J. Mol. Sci.* 23:3883. doi:10.3390/ijms23073883.

Bottaro, D.P., and L.A. Liotta. 2003. Cancer: Out of air is not out of action. *Nature*. 423:593–595. doi:10.1038/423593a.

Burnet, F.M. 1971. Immunological surveillance in neoplasia. *Transplant. Rev.* 7:3–25. doi:10.1111/j.1600-065x.1971.tb00461.x.

Burnet, M. 1964. IMMUNOLOGICAL FACTORS IN THE PROCESS OF CARCINOGENESIS. *Br. Med. Bull.* 20:154–158. doi:10.1093/oxfordjournals.bmb.a070310.

Campbell, M.J., F. Baehner, T. O'Meara, E. Ojukwu, B. Han, R. Mukhtar, V. Tandon, M. Endicott, Z. Zhu, J. Wong, G. Krings, A. Au, J.W. Gray, and L. Esserman. 2017. Characterizing the immune microenvironment in high-risk ductal carcinoma in situ of the breast. *Breast Cancer Res. Treat.* 161:17–28. doi:10.1007/s10549-016-4036-0.

Casasent, A.K., A. Schalck, R. Gao, E. Sei, A. Long, W. Pangburn, T. Casasent, F. Meric-Bernstam, M.E. Edgerton, and N.E. Navin. 2018. Multiclonal Invasion in Breast Tumors Identified by Topographic Single Cell Sequencing. *Cell*. 172:205-217.e12. doi:10.1016/j.cell.2017.12.007.

Chen, B., H. Wu, Y. Fang, G. Huang, C. Guo, C. Chen, L. He, Z. Chen, X. Hou, C. Li, and J. Wu. 2024. Prognostic implication of novel immune-related signature in breast cancer. *Medicine (Baltimore)*. 103:e37065. doi:10.1097/MD.0000000000037065.

Chen, X.-Y., A.A. Thike, N.D. Md Nasir, V.C.Y. Koh, B.H. Bay, and P.H. Tan. 2020. Higher density of stromal M2 macrophages in breast ductal carcinoma in situ predicts recurrence. *Virchows Arch.* 476:825–833. doi:10.1007/s00428-019-02735-1.

Cheung, K.J., E. Gabrielson, Z. Werb, and A.J. Ewald. 2013. Collective invasion in breast cancer requires a conserved basal epithelial program. *Cell*. 155:1639–1651. doi:10.1016/j.cell.2013.11.029.

Cheung, K.J., V. Padmanaban, V. Silvestri, K. Schipper, J.D. Cohen, A.N. Fairchild, M.A. Gorin, J.E. Verdone, K.J. Pienta, J.S. Bader, and A.J. Ewald. 2016. Polyclonal breast cancer metastases arise

from collective dissemination of keratin 14-expressing tumor cell clusters. *Proc. Natl. Acad. Sci. U. S. A.* 113:E854-863. doi:10.1073/pnas.1508541113.

Clark, A.G., and D.M. Vignjevic. 2015. Modes of cancer cell invasion and the role of the microenvironment. *Curr. Opin. Cell Biol.* 36:13–22. doi:10.1016/j.ceb.2015.06.004.

Cobleigh, M.A., S.J. Anderson, K.P. Siziopikou, D.W. Arthur, R. Rabinovitch, T.B. Julian, D.S. Parda, S.A. Seaward, D.L. Carter, J.A. Lyons, M.S. Dillmon, G.C. Magrinat, V.S. Kavadi, A.M. Zibelli, L. Tiriveedhi, M.L. Hill, M.K. Melnik, S. Beriwal, E.P. Mamounas, and N. Wolmark. 2021. Comparison of Radiation With or Without Concurrent Trastuzumab for HER2-Positive Ductal Carcinoma In Situ Resected by Lumpectomy: A Phase III Clinical Trial. *J. Clin. Oncol.* 39:2367–2374. doi:10.1200/JCO.20.02824.

Conklin, M.W., J.C. Eickhoff, K.M. Riching, C.A. Pehlke, K.W. Eliceiri, P.P. Provenzano, A. Friedl, and P.J. Keely. 2011. Aligned Collagen Is a Prognostic Signature for Survival in Human Breast Carcinoma. *Am. J. Pathol.* 178:1221–1232. doi:10.1016/j.ajpath.2010.11.076.

Conklin, M.W., R.E. Gangnon, B.L. Sprague, L. Van Gemert, J.M. Hampton, K.W. Eliceiri, J.S. Bredfeldt, Y. Liu, N. Surachaicharn, P.A. Newcomb, A. Friedl, P.J. Keely, and A. Trentham-Dietz. 2018. Collagen Alignment as a Predictor of Recurrence after Ductal Carcinoma In Situ. *Cancer Epidemiol. Biomarkers Prev.* 27:138–145. doi:10.1158/1055-9965.EPI-17-0720.

Cserni, G., and A. Sejben. 2020. Grading Ductal Carcinoma In Situ (DCIS) of the Breast – What's Wrong with It? *Pathol. Oncol. Res.* 26:665–671. doi:10.1007/s12253-019-00760-8.

Cunha, P.O.R., M. Ornstein, and J.L. Jones. 2010. Progression of Ductal Carcinoma in Situ from the Pathological Perspective. *Breast Care*. 5:233–239. doi:10.1159/000319625.

Cuzick, J., I. Sestak, S.E. Pinder, I.O. Ellis, S. Forsyth, N.J. Bundred, J.F. Forbes, H. Bishop, I.S. Fentiman, and W.D. George. 2011. Effect of tamoxifen and radiotherapy in women with locally excised ductal carcinoma in situ: long-term results from the UK/ANZ DCIS trial. *Lancet Oncol.* 12:21–29. doi:10.1016/S1470-2045(10)70266-7.

Dunne, C., J.P. Burke, M. Morrow, and M.R. Kell. 2009. Effect of margin status on local recurrence after breast conservation and radiation therapy for ductal carcinoma in situ. *J. Clin. Oncol. Off. J. Am. Soc. Clin. Oncol.* 27:1615–1620. doi:10.1200/JCO.2008.17.5182.

Emens, L.A., S. Adams, C.H. Barrios, V.C. Dieras, H. Iwata, S. Loi, H.S. Rugo, A. Schneeweiss, E.P. Winer, S. Patel, V. Henschel, A. Swat, M. Kaul, L. Molinero, S.Y. Chui, and P. Schmid. 2020. LBA16 IMpassion130: Final OS analysis from the pivotal phase III study of atezolizumab + nab-paclitaxel vs placebo + nab-paclitaxel in previously untreated locally advanced or metastatic triple-negative breast cancer. *Ann. Oncol.* 31:S1148. doi:10.1016/j.annonc.2020.08.2244.

Eng, L.G., S. Dawood, V. Sopik, B. Haaland, P.S. Tan, N. Bhoo-Pathy, E. Warner, J. Iqbal, S.A. Narod, and R. Dent. 2016. Ten-year survival in women with primary stage IV breast cancer. *Breast Cancer Res. Treat.* 160:145–152. doi:10.1007/s10549-016-3974-x.

Ernster, V.L., R. Ballard-Barbash, W.E. Barlow, Y. Zheng, D.L. Weaver, G. Cutter, B.C. Yankaskas, R. Rosenberg, P.A. Carney, K. Kerlikowske, S.H. Taplin, N. Urban, and B.M. Geller. 2002. Detection of ductal carcinoma in situ in women undergoing screening mammography. *J. Natl. Cancer Inst.* 94:1546–1554. doi:10.1093/jnci/94.20.1546.

Figueroa, J.D., R.M. Pfeiffer, D.A. Patel, L. Linville, L.A. Brinton, G.L. Gierach, X.R. Yang, D. Papathomas, D. Visscher, C. Mies, A.C. Degnim, W.F. Anderson, S. Hewitt, Z.G. Khodr, S.E. Clare, A.M. Storniolo, and M.E. Sherman. 2014. Terminal Duct Lobular Unit Involution of the Normal

Breast: Implications for Breast Cancer Etiology. *JNCI J. Natl. Cancer Inst.* 106:dju286. doi:10.1093/jnci/dju286.

Gibson, S.V., R.M. Roozitalab, M.D. Allen, J.L. Jones, E.P. Carter, and R.P. Grose. 2023. Everybody needs good neighbours: the progressive DCIS microenvironment. *Trends Cancer*. 9:326–338. doi:10.1016/j.trecan.2023.01.002.

Gil Del Alcazar, C.R., S.J. Huh, M.B. Ekram, A. Trinh, L.L. Liu, F. Beca, X. Zi, M. Kwak, H. Bergholtz, Y. Su, L. Ding, H.G. Russnes, A.L. Richardson, K. Babski, E. Min Hui Kim, C.H. McDonnell, J. Wagner, R. Rowberry, G.J. Freeman, D. Dillon, T. Sorlie, L.M. Coussens, J.E. Garber, R. Fan, K. Bobolis, D.C. Allred, J. Jeong, S.Y. Park, F. Michor, and K. Polyak. 2017. Immune Escape in Breast Cancer During In Situ to Invasive Carcinoma Transition. *Cancer Discov.* 7:1098–1115. doi:10.1158/2159-8290.CD-17-0222.

Goff, S.L., and D.N. Danforth. 2021. The Role of Immune Cells in Breast Tissue and Immunotherapy for the Treatment of Breast Cancer. *Clin. Breast Cancer*. 21:e63–e73. doi:10.1016/j.clbc.2020.06.011.

Gudjonsson, T., M.C. Adriance, M.D. Sternlicht, O.W. Petersen, and M.J. Bissell. 2005. Myoepithelial cells: their origin and function in breast morphogenesis and neoplasia. *J. Mammary Gland Biol. Neoplasia*. 10:261–272. doi:10.1007/s10911-005-9586-4.

Hanahan, D., and R.A. Weinberg. 2011. Hallmarks of cancer: the next generation. *Cell*. 144:646–674. doi:10.1016/j.cell.2011.02.013.

Heer, E., A. Harper, N. Escandor, H. Sung, V. McCormack, and M.M. Fidler-Benaoudia. 2020. Global burden and trends in premenopausal and postmenopausal breast cancer: a population-based study. *Lancet Glob. Health*. 8:e1027–e1037. doi:10.1016/S2214-109X(20)30215-1.

Hilson, J.B., S.J. Schnitt, and L.C. Collins. 2009. Phenotypic alterations in ductal carcinoma in situ-associated myoepithelial cells: biologic and diagnostic implications. *Am. J. Surg. Pathol.* 33:227–232. doi:10.1097/PAS.0b013e318180431d.

Holliger, P., and P.J. Hudson. 2005. Engineered antibody fragments and the rise of single domains. *Nat. Biotechnol.* 23:1126–1136. doi:10.1038/nbt1142.

Ibragimova, K.I.E., S.M.E. Geurts, D. Laczkó, M. Meegdes, F. Erdkamp, J.B. Heijns, J. Tol, B.E.P.J. Vriens, K.N.A. Aaldering, M.W. Dercksen, M.J.A.E. Pepels, N.A.J.B. Peters, L.M.H. van de Winkel, A.J. van de Wouw, A. de Fallois, M.A.C.E. van Kats, and V.C.G. Tjan-Heijnen. 2024. Trastuzumab Resistance in Patients With HER2-Positive Advanced Breast Cancer: Results From the SONABRE Registry. *Clin. Breast Cancer*. 24:103–111. doi:10.1016/j.clbc.2023.10.009.

Insua-Rodríguez, J., and T. Oskarsson. 2016. The extracellular matrix in breast cancer. *Adv. Drug Deliv. Rev.* 97:41–55. doi:10.1016/j.addr.2015.12.017.

Jääskeläinen, M.M., R. Tumelius, K. Hämäläinen, K. Rilla, S. Oikari, A. Rönkä, T. Selander, A. Mannermaa, S. Tiainen, and P. Auvinen. 2024. High Numbers of CD163+ Tumor-Associated Macrophages Predict Poor Prognosis in HER2+ Breast Cancer. *Cancers*. 16:634. doi:10.3390/cancers16030634.

Jahkola, T., T. Toivonen, S. Nordling, K. von Smitten, and I. Virtanen. 1998. Expression of tenascin-C in intraductal carcinoma of human breast: relationship to invasion. *Eur. J. Cancer Oxf. Engl. 1990*. 34:1687–1692. doi:10.1016/s0959-8049(98)00215-9.

Joensuu, H., P. Bono, V. Kataja, T. Alanko, R. Kokko, R. Asola, T. Utriainen, T. Turpeenniemi-Hujanen, S. Jyrkkiö, K. Möykkynen, L. Helle, S. Ingalsuo, M. Pajunen, M. Huusko, T. Salminen, P. Auvinen, H. Leinonen, M. Leinonen, J. Isola, and P.-L. Kellokumpu-Lehtinen. 2009. Fluorouracil, epirubicin, and cyclophosphamide with either docetaxel or vinorelbine, with or without trastuzumab, as

adjuvant treatments of breast cancer: final results of the FinHer Trial. *J. Clin. Oncol. Off. J. Am. Soc. Clin. Oncol.* 27:5685–5692. doi:10.1200/JCO.2008.21.4577.

Jukkola, A. 2024. Rintasyövän valtakunnallinen diagnostiikka- ja hoitosuositus. Finnish breast cancer group. 2024. p. 92.

Junttila, T.T., R.W. Akita, K. Parsons, C. Fields, G.D. Lewis Phillips, L.S. Friedman, D. Sampath, and M.X. Sliwkowski. 2009. Ligand-independent HER2/HER3/PI3K complex is disrupted by trastuzumab and is effectively inhibited by the PI3K inhibitor GDC-0941. *Cancer Cell*. 15:429–440. doi:10.1016/j.ccr.2009.03.020.

Köninki, K., M. Barok, M. Tanner, S. Staff, J. Pitkänen, P. Hemmilä, J. Ilvesaro, and J. Isola. 2010. Multiple molecular mechanisms underlying trastuzumab and lapatinib resistance in JIMT-1 breast cancer cells. *Cancer Lett.* 294:211–219. doi:10.1016/j.canlet.2010.02.002.

Kute, T., J.R. Stehle, Jr., D. Ornelles, N. Walker, O. Delbono, and J.P. Vaughn. 2012. Understanding key assay parameters that affect measurements of trastuzumab-mediated ADCC against Her2 positive breast cancer cells. *Oncoimmunology*. 1:810–821. doi:10.4161/onci.20447.

Łazarczyk, A., J. Streb, P. Hałubiec, A. Streb-Smoleń, R. Jach, D. Hodorowicz-Zaniewska, E. Łuczyńska, and J. Szpor. 2023. Neoductgenesis in Ductal Carcinoma In Situ Coexists with Morphological Abnormalities Characteristic for More Aggressive Tumor Biology. *Diagnostics*. 13:787. doi:10.3390/diagnostics13040787.

Lee-Hoeflich, S.T., L. Crocker, E. Yao, T. Pham, X. Munroe, K.P. Hoeflich, M.X. Sliwkowski, and H.M. Stern. 2008. A central role for HER3 in HER2-amplified breast cancer: implications for targeted therapy. *Cancer Res.* 68:5878–5887. doi:10.1158/0008-5472.CAN-08-0380.

Leek, R.D., C.E. Lewis, R. Whitehouse, M. Greenall, J. Clarke, and A.L. Harris. 1996. Association of macrophage infiltration with angiogenesis and prognosis in invasive breast carcinoma. *Cancer Res.* 56:4625–4629.

Leena Vehmanen. 2020. Rintasyövän hoito. *Lääkärikirja Duodecim*.

Lepucki, A., K. Orlińska, A. Mielczarek-Palacz, J. Kabut, P. Olczyk, and K. Komosińska-Vassev. 2022. The Role of Extracellular Matrix Proteins in Breast Cancer. *J. Clin. Med.* 11:1250. doi:10.3390/jcm11051250.

Li, H.-X., S.-Q. Wang, Z.-X. Lian, S.-L. Deng, and K. Yu. 2022. Relationship between Tumor Infiltrating Immune Cells and Tumor Metastasis and Its Prognostic Value in Cancer. *Cells*. 12:64. doi:10.3390/cells12010064.

Linde, N., M. Casanova-Acebes, M.S. Sosa, A. Mortha, A. Rahman, E. Farias, K. Harper, E. Tardio, I. Reyes Torres, J. Jones, J. Condeelis, M. Merad, and J.A. Aguirre-Ghiso. 2018. Macrophages orchestrate breast cancer early dissemination and metastasis. *Nat. Commun.* 9:21. doi:10.1038/s41467-017-02481-5.

Liu, Z., M. Li, Z. Jiang, and X. Wang. 2018. A Comprehensive Immunologic Portrait of Triple-Negative Breast Cancer. *Transl. Oncol.* 11:311–329. doi:10.1016/j.tranon.2018.01.011.

Loibl, S., F. André, T. Bachelot, C.H. Barrios, J. Bergh, H.J. Burstein, M.J. Cardoso, L.A. Carey, S. Dawood, L. Del Mastro, C. Denkert, E.M. Fallenberg, P.A. Francis, H. Gamal-Eldin, K. Gelmon, C.E. Geyer, M. Gnant, V. Guarneri, S. Gupta, S.B. Kim, D. Krug, M. Martin, I. Meattini, M. Morrow, W. Janni, S. Paluch-Shimon, A. Partridge, P. Poortmans, L. Pusztai, M.M. Regan, J. Sparano, T. Spanic, S. Swain, S. Tjulandin, M. Toi, D. Trapani, A. Tutt, B. Xu, G. Curigliano, N. Harbeck, and ESMO Guidelines Committee. Electronic address: clinicalguidelines@esmo.org. 2024.

Early breast cancer: ESMO Clinical Practice Guideline for diagnosis, treatment and follow-up. *Ann. Oncol. Off. J. Eur. Soc. Med. Oncol.* 35:159–182. doi:10.1016/j.annonc.2023.11.016.

Loibl, S., and L. Gianni. 2017. HER2-positive breast cancer. *The Lancet*. 389:2415–2429. doi:10.1016/S0140-6736(16)32417-5.

Macià, F., M. Porta, C. Murta-Nascimento, S. Servitja, M. Guxens, A. Burón, I. Tusquets, J. Albanell, and X. Castells. 2012. Factors affecting 5- and 10-year survival of women with breast cancer: An analysis based on a public general hospital in Barcelona. *Cancer Epidemiol.* 36:554–559. doi:10.1016/j.canep.2012.07.003.

Martínez-Pérez, C., A.K. Turnbull, G.E. Ekatah, L.M. Arthur, A.H. Sims, J.S. Thomas, and J.M. Dixon. 2017. Current treatment trends and the need for better predictive tools in the management of ductal carcinoma in situ of the breast. *Cancer Treat. Rev.* 55:163–172. doi:10.1016/j.ctrv.2017.03.009.

McInroy, L., and A. Määttä. 2007. Down-regulation of vimentin expression inhibits carcinoma cell migration and adhesion. *Biochem. Biophys. Res. Commun.* 360:109–114. doi:10.1016/j.bbrc.2007.06.036.

Mendez, M.G., S.-I. Kojima, and R.D. Goldman. 2010. Vimentin induces changes in cell shape, motility, and adhesion during the epithelial to mesenchymal transition. *FASEB J.* 24:1838–1851. doi:10.1096/fj.09-151639.

Miligy, I.M., M.S. Toss, K.L. Gorringe, A.H.S. Lee, I.O. Ellis, A.R. Green, and E.A. Rakha. 2019. The clinical and biological significance of HER2 over-expression in breast ductal carcinoma in situ: a large study from a single institution. *Br. J. Cancer*. 120:1075–1082. doi:10.1038/s41416-019-0436-3.

Morrow, M., K.J. Van Zee, L.J. Solin, N. Houssami, M. Chavez-MacGregor, J.R. Harris, J. Horton, S. Hwang, P.L. Johnson, M.L. Marinovich, S.J. Schnitt, I. Wapnir, and M.S. Moran. 2016. Society of Surgical Oncology-American Society for Radiation Oncology-American Society of Clinical Oncology Consensus Guideline on Margins for Breast-Conserving Surgery With Whole-Breast Irradiation in Ductal Carcinoma In Situ. *J. Clin. Oncol. Off. J. Am. Soc. Clin. Oncol.* 34:4040–4046. doi:10.1200/JCO.2016.68.3573.

Nagata, Y., K.-H. Lan, X. Zhou, M. Tan, F.J. Esteva, A.A. Sahin, K.S. Klos, P. Li, B.P. Monia, N.T. Nguyen, G.N. Hortobagyi, M.-C. Hung, and D. Yu. 2004. PTEN activation contributes to tumor inhibition by trastuzumab, and loss of PTEN predicts trastuzumab resistance in patients. *Cancer Cell*. 6:117–127. doi:10.1016/j.ccr.2004.06.022.

Nathanson, S.D., M. Detmar, T.P. Padera, L.R. Yates, D.R. Welch, T.C. Beadnell, A.D. Scheid, E.D. Wrenn, and K. Cheung. 2022. Mechanisms of breast cancer metastasis. *Clin. Exp. Metastasis*. 39:117–137. doi:10.1007/s10585-021-10090-2.

Orrantia-Borunda, E., P. Anchondo-Nuñez, L.E. Acuña-Aguilar, F.O. Gómez-Valles, and C.A. Ramírez-Valdespino. 2022. Subtypes of Breast Cancer. *In* Breast Cancer. H.N. Mayrovitz, editor. Exon Publications, Brisbane (AU).

Oskarsson, T., S. Acharyya, X.H.-F. Zhang, S. Vanharanta, S.F. Tavazoie, P.G. Morris, R.J. Downey, K. Manova-Todorova, E. Brogi, and J. Massagué. 2011. Breast cancer cells produce tenascin C as a metastatic niche component to colonize the lungs. *Nat. Med.* 17:867–874. doi:10.1038/nm.2379.

Papanicolaou, M., A.L. Parker, M. Yam, E.C. Filipe, S.Z. Wu, J.L. Chitty, K. Wyllie, E. Tran, E. Mok, A. Nadalini, J.N. Skhinas, M.C. Lucas, D. Herrmann, M. Nobis, B.A. Pereira, A.M.K. Law, L. Castillo, K.J. Murphy, A. Zaratzian, J.F. Hastings, D.R. Croucher, E. Lim, B.G. Oliver, F.V. Mora, B.L. Parker, D. Gallego-Ortega, A. Swarbrick, S. O'Toole, P. Timpson, and T.R. Cox. 2022. Temporal

profiling of the breast tumour microenvironment reveals collagen XII as a driver of metastasis. *Nat. Commun.* 13:4587. doi:10.1038/s41467-022-32255-7.

Peurla, M., O. Paavolainen, E. Tammelin, S.-R. Sulander, L. Mourao, P. Boström, N. Brück, C.L. Scheele, P. Hartiala, and E. Peuhu. 2023. Morphometric analysis of the terminal ductal lobular unit architecture in human breast. 2023.03.12.532249. doi:10.1101/2023.03.12.532249.

Pietilä, M., P. Sahgal, E. Peuhu, N.Z. Jäntti, I. Paatero, E. Närvä, H. Al-Akhrass, J. Lilja, M. Georgiadou, O.M. Andersen, A. Padzik, H. Sihto, H. Joensuu, M. Blomqvist, I. Saarinen, P.J. Boström, P. Taimen, and J. Ivaska. 2019. SORLA regulates endosomal trafficking and oncogenic fitness of HER2. *Nat. Commun.* 10:2340. doi:10.1038/s41467-019-10275-0.

Pruneri, G., M. Lazzeroni, V. Bagnardi, G.B. Tiburzio, N. Rotmensz, A. DeCensi, A. Guerrieri-Gonzaga, A. Vingiani, G. Curigliano, S. Zurrida, F. Bassi, R. Salgado, G. Van den Eynden, S. Loi, C. Denkert, B. Bonanni, and G. Viale. 2017. The prevalence and clinical relevance of tumor-infiltrating lymphocytes (TILs) in ductal carcinoma in situ of the breast. *Ann. Oncol. Off. J. Eur. Soc. Med. Oncol.* 28:321–328. doi:10.1093/annonc/mdw623.

Rakha, E.A., G.M. Tse, and C.M. Quinn. 2023. An update on the pathological classification of breast cancer. *Histopathology*. 82:5–16. doi:10.1111/his.14786.

Risom, T., D.R. Glass, I. Averbukh, C.C. Liu, A. Baranski, A. Kagel, E.F. McCaffrey, N.F. Greenwald, B. Rivero-Gutiérrez, S.H. Strand, S. Varma, A. Kong, L. Keren, S. Srivastava, C. Zhu, Z. Khair, D.J. Veis, K. Deschryver, S. Vennam, C. Maley, E.S. Hwang, J.R. Marks, S.C. Bendall, G.A. Colditz, R.B. West, and M. Angelo. 2022. Transition to invasive breast cancer is associated with progressive changes in the structure and composition of tumor stroma. *Cell*. 185:299-310.e18. doi:10.1016/j.cell.2021.12.023.

Romond, E.H., E.A. Perez, J. Bryant, V.J. Suman, C.E. Geyer, N.E. Davidson, E. Tan-Chiu, S. Martino, S. Paik, P.A. Kaufman, S.M. Swain, T.M. Pisansky, L. Fehrenbacher, L.A. Kutteh, V.G. Vogel, D.W. Visscher, G. Yothers, R.B. Jenkins, A.M. Brown, S.R. Dakhil, E.P. Mamounas, W.L. Lingle, P.M. Klein, J.N. Ingle, and N. Wolmark. 2005. Trastuzumab plus adjuvant chemotherapy for operable HER2-positive breast cancer. *N. Engl. J. Med.* 353:1673–1684. doi:10.1056/NEJMoa052122.

Rubin, I., and Y. Yarden. 2001. The basic biology of HER2. *Ann. Oncol.* 12:S3–S8. doi:10.1093/annonc/12.suppl_1.S3.

Shinohara, H., M. Kobayashi, K. Hayashi, D. Nogawa, A. Asakawa, Y. Ohata, K. Kubota, H. Takahashi, M. Yamada, M. Tokunaga, Y. Kinugasa, G. Oda, T. Nakagawa, I. Onishi, Y. Kinowaki, M. Kurata, K. Ohashi, M. Kitagawa, and K. Yamamoto. 2022. Spatial and Quantitative Analysis of Tumor-Associated Macrophages: Intratumoral CD163-/PD-L1+ TAMs as a Marker of Favorable Clinical Outcomes in Triple-Negative Breast Cancer. *Int. J. Mol. Sci.* 23:13235. doi:10.3390/ijms232113235.

Sirka, O.K., E.R. Shamir, and A.J. Ewald. 2018. Myoepithelial cells are a dynamic barrier to epithelial dissemination. *J. Cell Biol.* 217:3368–3381. doi:10.1083/jcb.201802144.

Slamon, D.J., G.M. Clark, S.G. Wong, W.J. Levin, A. Ullrich, and W.L. McGuire. 1987. Human Breast Cancer: Correlation of Relapse and Survival with Amplification of the HER-2/ *neu* Oncogene. *Science*. 235:177–182. doi:10.1126/science.3798106.

Slamon, D.J., B. Leyland-Jones, S. Shak, H. Fuchs, V. Paton, A. Bajamonde, T. Fleming, W. Eiermann, J. Wolter, M. Pegram, J. Baselga, and L. Norton. 2001. Use of Chemotherapy plus a Monoclonal Antibody against HER2 for Metastatic Breast Cancer That Overexpresses HER2. *N. Engl. J. Med.* 344:783–792. doi:10.1056/NEJM200103153441101.

Stanton, S.E., S. Adams, and M.L. Disis. 2016. Variation in the Incidence and Magnitude of Tumor-Infiltrating Lymphocytes in Breast Cancer Subtypes: A Systematic Review. *JAMA Oncol.* 2:1354–1360. doi:10.1001/jamaoncol.2016.1061.

Tabár, L., P.B. Dean, F. Lee Tucker, A.M.-F. Yen, R.W.-J. Chang, C.-Y. Hsu, R.A. Smith, S.W. Duffy, and T.H.-H. Chen. 2022. Breast cancers originating from the major lactiferous ducts and the process of neoductgenesis: Ductal Adenocarcinoma of the Breast, DAB. *Eur. J. Radiol.* 153:110363. doi:10.1016/j.ejrad.2022.110363.

Tabar, L., H.-H. Tony Chen, M.F. Amy Yen, T. Tot, T.-H. Tung, L.-S. Chen, Y.-H. Chiu, S.W. Duffy, and R.A. Smith. 2004. Mammographic tumor features can predict long-term outcomes reliably in women with 1-14-mm invasive breast carcinoma. *Cancer*. 101:1745–1759. doi:10.1002/cncr.20582.

Tanner, M., A.I. Kapanen, T. Junttila, O. Raheem, S. Grenman, J. Elo, K. Elenius, and J. Isola. 2005. Characterization of a novel cell line established from a patient with Herceptin-resistant breast cancer. *Mol. Cancer Ther.* 3:1585–1592. doi:10.1158/1535-7163.1585.3.12.

Teo, N.B., B.S. Shoker, C. Jarvis, L. Martin, J.P. Sloane, and C. Holcombe. 2003. Angiogenesis and invasive recurrence in ductal carcinoma in situ of the breast. *Eur. J. Cancer*. 39:38–44. doi:10.1016/S0959-8049(02)00248-4.

Thompson, E., J.M. Taube, H. Elwood, R. Sharma, A. Meeker, H.N. Warzecha, P. Argani, A. Cimino-Mathews, and L.A. Emens. 2016. The Immune Microenvironment of Breast Ductal Carcinoma in Situ. *Mod. Pathol. Off. J. U. S. Can. Acad. Pathol. Inc*. 29:249–258. doi:10.1038/modpathol.2015.158.

Thorat, M.A., P.M. Levey, J.L. Jones, S.E. Pinder, N.J. Bundred, I.S. Fentiman, and J. Cuzick. 2021. Prognostic and Predictive Value of HER2 Expression in Ductal Carcinoma In Situ: Results from the UK/ANZ DCIS Randomized Trial. *Clin. Cancer Res.* 27:5317–5324. doi:10.1158/1078-0432.CCR-21-1239.

Tomlinson-Hansen, S., M. Khan, and S. Cassaro. 2023. Breast Ductal Carcinoma in Situ. *In* StatPearls. StatPearls Publishing, Treasure Island (FL).

Toss, M.S., I. Miligy, A. Al-Kawaz, M. Alsleem, H. Khout, P.C. Rida, R. Aneja, A.R. Green, I.O. Ellis, and E.A. Rakha. 2018. Prognostic significance of tumor-infiltrating lymphocytes in ductal carcinoma in situ of the breast. *Mod. Pathol.* 31:1226–1236. doi:10.1038/s41379-018-0040-8.

Walker, R.A. 2001. The complexities of breast cancer desmoplasia. *Breast Cancer Res.* 3:143–145. doi:10.1186/bcr287.

Wang, J., B. Li, M. Luo, J. Huang, K. Zhang, S. Zheng, S. Zhang, and J. Zhou. 2024. Progression from ductal carcinoma in situ to invasive breast cancer: molecular features and clinical significance. *Signal Transduct. Target. Ther.* 9:1–28. doi:10.1038/s41392-024-01779-3.

Wang, J., and S.-G. Wu. 2023. Breast Cancer: An Overview of Current Therapeutic Strategies, Challenge, and Perspectives. *Breast Cancer Targets Ther.* 15:721–730. doi:10.2147/BCTT.S432526.

Wang, W., W. Zhu, F. Du, Y. Luo, and B. Xu. 2017. The Demographic Features, Clinicopathological Characteristics and Cancer-specific Outcomes for Patients with Microinvasive Breast Cancer: A SEER Database Analysis. *Sci. Rep.* 7:42045. doi:10.1038/srep42045.

Wang, Z., Z. Zheng, S. Jia, S. Liu, X. Xiao, G. Chen, W. Liang, and X. Lu. 2022. Trastuzumab resistance in HER2-positive breast cancer: Mechanisms, emerging biomarkers and targeting agents. *Front. Oncol.* 12:1006429. doi:10.3389/fonc.2022.1006429.

Wapnir, I.L., J.J. Dignam, B. Fisher, E.P. Mamounas, S.J. Anderson, T.B. Julian, S.R. Land, R.G. Margolese, S.M. Swain, J.P. Costantino, and N. Wolmark. 2011. Long-term outcomes of invasive ipsilateral breast tumor recurrences after lumpectomy in NSABP B-17 and B-24 randomized clinical trials for DCIS. *J. Natl. Cancer Inst.* 103:478–488. doi:10.1093/jnci/djr027.

Wawrzyniak, D., M. Grabowska, P. Głodowicz, K. Kuczyński, B. Kuczyńska, A. Fedoruk-Wyszomirska, and K. Rolle. 2020. Down-regulation of tenascin-C inhibits breast cancer cells development by cell growth, migration, and adhesion impairment. *PLoS ONE*. 15:e0237889. doi:10.1371/journal.pone.0237889.

Weis, S.M., and D.A. Cheresh. 2005. Pathophysiological consequences of VEGF-induced vascular permeability. *Nature*. 437:497–504. doi:10.1038/nature03987.

Weis, S.M., and D.A. Cheresh. 2011. Tumor angiogenesis: molecular pathways and therapeutic targets. *Nat. Med.* 17:1359–1370. doi:10.1038/nm.2537.

Wellings, S.R., H.M. Jensen, and R.G. Marcum. 1975. An Atlas of Subgross Pathology of the Human Breast With Special Reference to Possible Precancerous Lesions2. *JNCI J. Natl. Cancer Inst.* 55:231–273. doi:10.1093/jnci/55.2.231.

Werling, R.W., H. Hwang, H. Yaziji, and A.M. Gown. 2003. Immunohistochemical distinction of invasive from noninvasive breast lesions: a comparative study of p63 versus calponin and smooth muscle myosin heavy chain. *Am. J. Surg. Pathol.* 27:82–90. doi:10.1097/00000478-200301000-00009.

Wülfing, P., C. Kersting, H. Buerger, B. Mattsson, R. Mesters, C. Gustmann, B. Hinrichs, J. Tio, W. Böcker, and L. Kiesel. 2005. Expression patterns of angiogenic and lymphangiogenic factors in ductal breast carcinoma in situ. *Br. J. Cancer*. 92:1720–1728. doi:10.1038/sj.bjc.6602567.

Yang, L., Y. Li, E. Shen, F. Cao, L. Li, X. Li, X. Wang, S. Kariminia, B. Chang, H. Li, and Q. Li. 2017. NRG1-dependent activation of HER3 induces primary resistance to trastuzumab in HER2-overexpressing breast cancer cells. *Int. J. Oncol.* 51:1553–1562. doi:10.3892/ijo.2017.4130.

Yokota, T., D.E. Milenic, M. Whitlow, and J. Schlom. 1992. Rapid tumor penetration of a single-chain Fv and comparison with other immunoglobulin forms. *Cancer Res.* 52:3402–3408.

Yu, X., L. Wang, Y. Shen, C. Wang, Y. Zhang, Y. Meng, Y. Yang, B. Liang, B. Zhou, H. Wang, H. Wei, C. Lei, S. Hu, and B. Li. 2017. Targeting EGFR/HER2 heterodimerization with a novel anti-HER2 domain II/III antibody. *Mol. Immunol.* 87:300–307. doi:10.1016/j.molimm.2017.05.010.

Zazo, S., P. González-Alonso, E. Martín-Aparicio, C. Chamizo, I. Cristóbal, O. Arpí, A. Rovira, J. Albanell, P. Eroles, A. Lluch, J. Madoz-Gúrpide, and F. Rojo. 2016. Generation, characterization, and maintenance of trastuzumab-resistant HER2+ breast cancer cell lines. *Am. J. Cancer Res.* 6:2661–2678.

Zhang, J., D. Huang, P.E. Saw, and E. Song. 2022. Turning cold tumors hot: from molecular mechanisms to clinical applications. *Trends Immunol.* 43:523–545. doi:10.1016/j.it.2022.04.010.

Zhou, W., T. Sollie, T. Tot, C. Blomqvist, S. Abdsaleh, G. Liljegren, and F. Wärnberg. 2017. Ductal Breast Carcinoma In Situ: Mammographic Features and Its Relation to Prognosis and Tumour Biology in a Population Based Cohort. *Int. J. Breast Cancer*. 2017:4351319. doi:10.1155/2017/4351319.

Zhou, W., T. Sollie, T. Tot, S.E. Pinder, R.-M. Amini, C. Blomqvist, M.-L. Fjällskog, G. Christensson, S. Abdsaleh, and F. Wärnberg. 2014. Breast cancer with neoductgenesis: histopathological criteria and its correlation with mammographic and tumour features. *Int. J. Breast Cancer*. 2014:581706. doi:10.1155/2014/581706.